DEVELOPMENT OF JOINING TECHNIQUES FOR CARBON FIBER BASED POLYMER MATRIX COMPOSITES

A Thesis Submitted to
the Graduate School of
İzmir Institute of Technology
in Partial Fulfillment of the Requirements for the Degree of

MASTER OF SCIENCE

in Mechanical Engineering

by
Hande İPLİKÇİ

July 2022
İZMİR

ACKNOWLEDGMENTS

I would like to give my sincere thanks to my advisor, Prof. Metin TANOĞLU for his guidance, support, motivation, and encouragement during my thesis. Also, I would like to thank the thesis jury members for their interest.

Besides, this dissertation was supported by Tubitak project number 218M801. I would like to thank the rest of my Tubitak project committee members Assoc. Prof. Engin AKTAŞ and Assoc. Prof. Murat BARIŞIK for their encouragement and constructive comments.

Also, I would like to thank Turkish Aerospace Industries Inc. (TUSAŞ) of Turkey for providing film adhesive, unidirectional carbon plates.

And also, I would like to thank IZTECH Center for Materials Research (MAM) for their contribution to the analysis in this thesis.

My laboratory friends who helped and supported me throughout my Master's Education; I would like to thank Ceren TÜRKDOĞAN, Gözde ESENOĞLU, Seçkin MARTİN and Nazife ÇERÇİ.

Finally, and most importantly, I dedicate this thesis to my beloved family for their love, patience and support throughout my life. I would like to thank my dear father Sinan Hakan İPLİKÇİ, my dear mother Nurdan İPLİKÇİ and my dear little brother Metin Yiğit İplikçi for everything. My dear family, I am grateful to you for raising me to be a free and good individual in every sense. I will always make you proud.

ABSTRACT

DEVELOPMENT OF JOINING TECHNIQUES FOR CARBON FIBER BASED POLYMER MATRIX COMPOSITES

In recent years, adhesive bonding has been a promising joining technology for CFRP composites. An appropriate treatment of surfaces for adhesive bonding is one of the effective factors for obtaining a high-quality adhesion strength. However, the adhesion strength is decreased by contaminants, like release agents, as well as an excess of matrix in the top layer. The contact of the adhesive with the reinforcing element is critical. Therefore, it is necessary to make a pre-preparation process on the adherent surface.

One of the surface treatments preferred due to the advantages it provides is laser processing. The joint area strength of CFRP (carbon fiber reinforced polymer) composite can be enhanced with laser surface treatment. In this work, the carbon fiber/epoxy composites surface treatment by a nanosecond (1064nm wavelength) laser has been investigated. The polymer layer (epoxy matrix) on the CFRP (carbon fiber reinforced polymer) composite surface was selectively removed by laser treatment to expose carbon fibers. In order to remove the epoxy from the surface sufficiently, laser surface modification parameters were investigated and their effects were examined. These parameters are laser power, frequency, scanning speed and offset distance, respectively. Epoxy removal and fibers damage was analyzed by optical microscope and SEM (scanning electron microscope). Contact angle tests were carried out to analyzed wettability effect on the laser parameters. Lap shear, charpy impact and double cantilever beam (DCB) tests were performed to examine the effect of laser surface modification on mechanical performance.

ÖZET

KARBON FİBER ESASLI POLİMER MATRİKS KOMPOZİTLER İÇİN BİRLEŞTİRME TEKNİKLERİNİN GELİŞTİRİLMESİ

Son yıllarda yapıştırıcıyla birleşme, CFRP (karbon fiber takviyeli polimer) kompozit için umut verici bir birleştirme teknolojisi olmuştur. Yapıştırma için yüzeylerin uygun şekilde işlenmesi, yüksek kaliteli bir yapışma mukavemeti elde etmek için etkili faktörlerden biridir. Bununla birlikte, yapışma kuvveti, ayırıcı maddeler gibi kirleticiler veya üst katmandaki fazla matris yüzünden azalır. Yapıştırıcının takviye elemanı ile teması çok önemlidir. Bu nedenle birleştirme bölgesinin yüzeyinde bir ön hazırlık işlemi yapılması gerekmektedir.

Sağladığı avantajlar nedeniyle tercih edilen yüzey işlemlerinden biri de lazer ablasyon işlemedir. CFRP kompozitin birleşme bölgesi mukavemeti, lazer yüzey işlemi ile arttırılabilir. Bu çalışmada, karbon fiber/epoksi kompozitlerin nanosaniye (1064 nm dalga boyu) lazer ile yüzey işlemi incelenmiştir. CFRP (karbon fiber takviyeli polimer) kompozit yüzey üzerindeki polimer tabakası (epoksi matris), karbon fiberlere zarar vermeden açığa çıkarmak için lazer yüzey modifikasyonu ile seçici olarak uzaklaştırıldı. Yüzeyden epoksiyi yeterli derecede uzaklaştırmak için lazer yüzey modifikasyon parametreleri araştırıldı ve etkileri incelendi. Bu paremetreler sırasıyla güç, frekans, tarama hızı ve ofset mesafesidir. Epoksi uzaklaştırma ve lif hasarı optik mikroskop ve SEM (taramalı elektron mikroskobu) ile analiz edildi. Lazer parametreleri üzerindeki ıslanabilirlik etkisini analiz etmek için temas açısı testleri yapıldı. Lazer yüzey modifikasyonunun mekanik performansa etkisini incelemek için lap shear, charpy darbe ve çift konsol kiriş (DCB) testleri yapıldı.

Dedicated to my family.

TABLE OF CONTENTS

LIST OF FIGURES

Figure **Page**

Figure **Page**

Figure **Page**

LIST OF TABLES

LIST OF SYMBOLS AND ABBREVIATIONS

R	rate of crosshead motion, mm [in.]/min
L	support span, mm [in.]
d	depth of beam, mm [in.]
Z	rate of straining of the outer fiber, [in./ in./min]
s	stress in the outer fibers at midpoint, MPa [psi]
P	load N [lbf]
b	width, mm [in.]
ε_f	strain in the outer surface, mm/mm [in./in.],
D	maximum deflection of the center of the beam, mm [in.]
m	slope of the tangent N/mm [lbf/in.]
L'	half width of loading block.
N	loading block correction factor.
t	distance from the loading block pin to the centerline of the upper sample arm.
$\|\Delta\|$	effective delamination extension to correct for rotation of DCB arms at delamination front.
α	delamination length.
δ	load point deflection.
GI	opening Mode I interlaminar fracture toughness.
DCB	double cantilever beam
UD	unidirectional

CHAPTER 1

INTRODUCTION

1.1. Composite Materials

A composite material is a combination of two materials with different physical and chemical properties. Various positive properties are expected from a material at the same time. Unfortunately, materials may not show all the desired properties on their own. In an area where a high performance material is needed, strength, abrasion resistance, rigidity, impact resistance and lightness can be requested at the same time. These properties are difficult to achieve with only metals, only ceramics or only polymers. In such a case, the expectations can be met by combining and producing materials, each of which is good with a certain feature, to form a phase of the composite. In composite materials, there is a reinforcing material as the core and a matrix material forming the majority by volume.

The reinforcing material provides the strength and load-bearing properties of the composite material. Matrix material, on the other hand, prevents crack propagation that may occur in the transition to plastic deformation and delays the rupture of the composite material. Composites, especially polymer composites, have been extensively used in many structural applications because of their high strength and stiffness at low weight and good corrosion-resistance and fatigue properties. It provides many advantages with its features such as stability, hardness, resistance to abrasion. In addition, composite materials are almost as durable and hard as metals, as well as very light. There are two basic phases in a composite, namely the matrix and the reinforcement phase. The properties of these two elements can be controlled to meet the required qualifications.

One of the composite types is polymer matrix composites. A polymer matrix composite composed of a variety of short or continuous fibers bound together by a polymer matrix. The word polymer means many parts. Polymer materials are mostly

composed of carbon, hydrogen and other non-metal organic elements. Organic polymers form the main material of plastics. These are usually large molecule organic compounds. When examined chemically, it is seen that there is generally carbon (C), hydrogen (H), nitrogen (N), oxygen (O) elements in plastics. When these elements react with various methods, very large and complex molecules called macromolecules are formed and thus polymers are formed. The main fiber types used in composite materials are; Glass fiber, Carbon (Graphite) fiber, (PAN -polyacrylonitrile- and pitch origin), Aramid (Aromatic Polyamide) fiber, (Trade name: Kevlar-DuPont), Boron fiber, Oxide fiber, High density polyethylene fiber, Polyamide fiber, Polyester fiber, Natural organic fibers, Ceramic fibers[1–3].

Figure 1. 1. Composite materials in industry

Carbon fiber is a thread-like substance that comes from the Arabic language and is a technology product. Its main compositions are carbonized acrylic fiber (Orlon), tar and nylon. Although the structure of carbon fiber is 4.5 times lighter than steel, it is 3 times more durable. The aerospace industry has undergone a transformation from a metal-driven world to a composite-dominated new standard. The carbon fiber reinforced polymer (CFRP) composites are widely used in the aviation industry due to their properties such as lightweight, corrosion performance, durability, impact resistance, high mechanical strength and modulus[4–6].

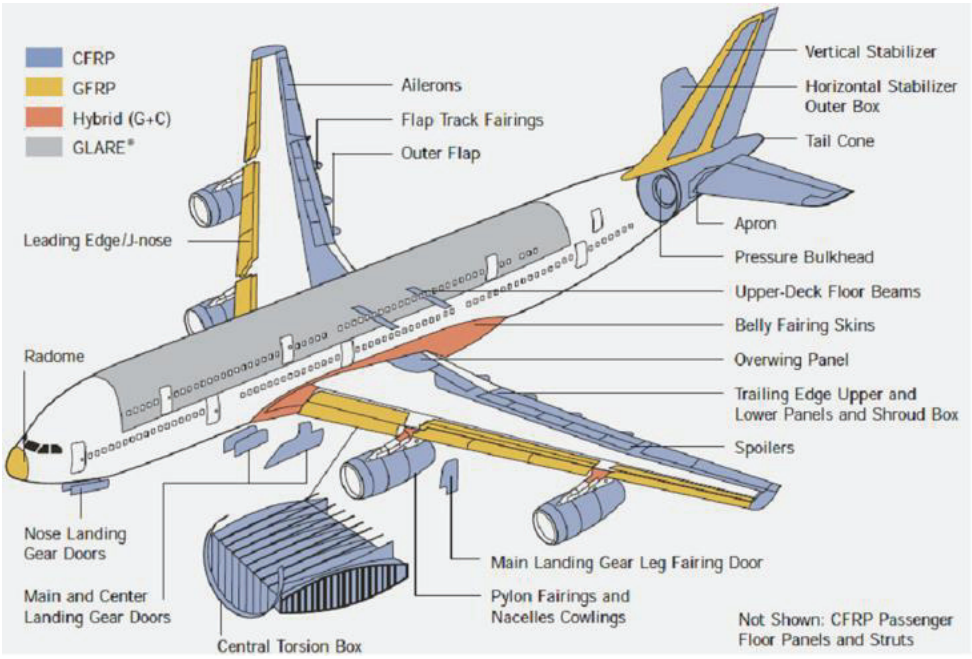

Figure 1. 2. Applications of fiber reinforced composites in Airbus A380 (Source: www.airporttech.tc.faa.gov).

1.2. Combination Methods for Structural Composite Parts

The adhesive bonding method is used as an alternative to mechanical connections in increasing engineering applications. It is faster than traditional connection methods and has many advantages. These advantages include lower structural weight, lower fabrication cost and improved damage tolerance[7,8]. The joining ability of the parts connected by the bonding method is improved and it is easy to apply. To obtain a strong and resistant adhesive bond; There must be an appropriate degree of adhesion between the adhesive and the bonding pad. However, the strength and durability of the adhesive, the compatibility of the adhesive with the surface, the bonding thickness, pollution, stress and environmental conditions affect the bonding quality and strength [9–11].

However, it should be noted that stress concentrations are still present in the adhesive and bonded materials due to the natural discontinuity of the materials in the bonding zone. It has been proven that the highest stresses in materials occur mostly

around the joint zone [12]. The stresses in the adhesive and on the bonded surfaces are divided into two as shear stress and peel stress according to the type of movement. For adhesive joints used to join developed composite materials, the peel stress is applied directly in the direction of the weak region of the matrix of the material, thus having a very significant effect on the bond strength. Often, the load-bearing ability of a composite structure is governed by the weakest stressed regions [13,14].

Success of bonding depends on the adhesion between the adhesive and the adherent such that the surface condition of the CFRP becomes the determining factor. Different surface treatment methods are used to increase the adhesion performance of composite materials. Surface impurities, smooth surfaces, low surface energies and wettability from the manufacturing process impair the adhesive behavior of composites. Prior to joining process, a clean surface with increased wettability is required to increase the adhesion capacity between CFRP and adhesive. Moreover, the resin at the outer surface of laminates needs to be removed in order to allow adhesive to bind directly to the load-carrying carbon fibers, not to filler resin above and around the fiber structures [9–11].

The use of adhesives for joining composite structures is increasing day by day due to its superior properties such as high bond strength, improved stress distribution and joining multi-material mixed structures [15]. In addition, adhesive bonding allows structures to be repaired using small composite parts, and these repairs can be made without much damage to the part [16]. The adhesive bonding method provides a continuous and considerably larger bonding area, which significantly reduces the stress intensity compared to mechanical fasteners [12].

Two of the most important disadvantages of mechanical fasteners are that they add weight and act as a stress concentrator in the material. The reasons for being a stress concentrator can be listed as follows; It deteriorates the structural quality of the components and causes layer separation. Alternative joining methods have become more important day by day, especially in the aviation industry, due to the effects of the disadvantages of mechanical fasteners [17]. Adhesive bonding techniques, one of the alternative joining methods, are shown in Figure 1.3. Co-curing is the simultaneous cure

of two parts in contact. The biggest reason why the co curing method is preferred is that the production and bonding of large and complicated parts can be done at the same time. The integration and stability of the part can be improved, labor costs and energy use can be decreased, manufacturing can be sped up, and all of these factors contribute to cost and energy reduction [18]. Co-bonding is the process where a cured structure is laid up against an uncured laminate with an adhesive at the interface. Secondary bonding is the adhesive joining of two precured parts [19].

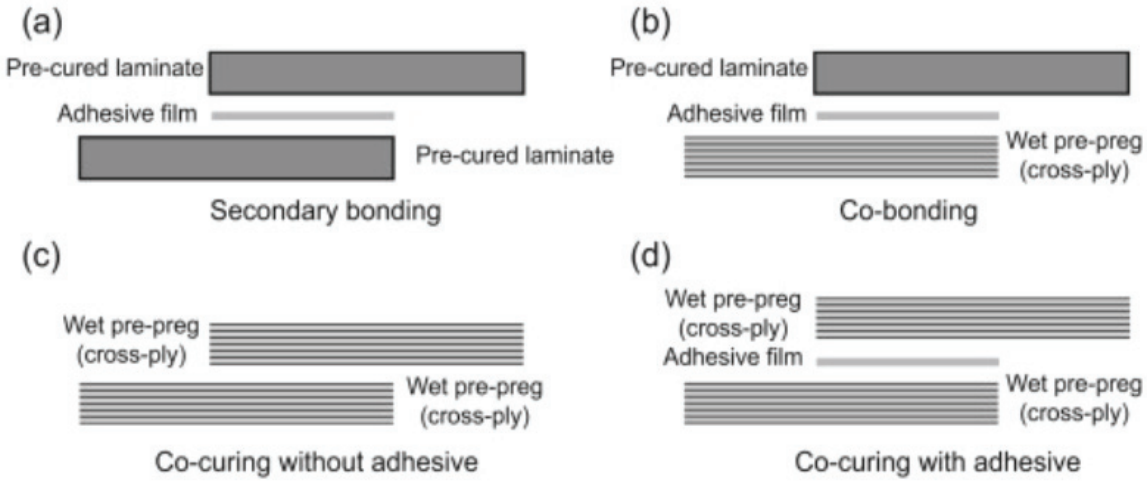

Figure 1. 3. Schematic of the joining methods
(Source: R.D.S.G. Campilho et al., 2015 [17])

Adhesive bonds techniques have a total of six fracture mechanisms, but usually two of those generally observed. Cohesive and adhesive fractures are two different types of fracture processes. In Figure 1.4, the types of failure of the adhesive joint are show and they are (a) adhesive failure, (b) cohesive failure, (c) thin-layer cohesive failure (d) fiber-tear failure, (e) light-tear failure and (f) stock-break failure. If the adhesive failure mechanism is exhibited, it is a failed adhesive joining method. Between the adhesive and one of the adhered ones, these failures take place. In bonded structures where adhesion is poor, various failure mechanisms typically take place [20,21]. Failure modes more significant than the maximum load in the samples that were adhered together. They also demonstrated how crucial it is to treat the adherents' surfaces to ensure good adhesion[22].

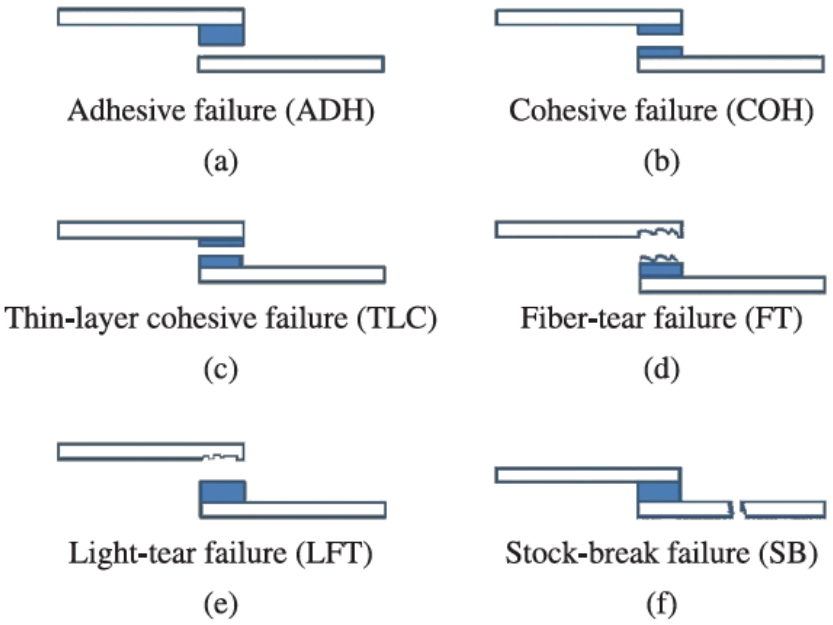

Figure 1. 4. Representation of failure modes characteristic of adhesive joints submitted to shearing (Source: Quini and Marinucci, 2021[23]).

1.3. Surface Treatment Methods

Various forms of surface treatments have been utilized to enhance the adhesion of the material systems [6]. In general, surface treatments applied to CFRP parts are divided into two main groups. First group contains is, chemical processes such as photografting and surface functionalization have been used to treat the surface [7,24], however its harm to the environment is high due to the waste generated by these methods, and these processes are not suitable for automation. The other one consists of, mechanical treatments such as peel-ply and grit-blasting methods [5,8], however these methods have disadvantages such as surface contamination, impracticality and time loss (Figure 1.5). Instead, recent studies have presented the laser surface treatment as a good option due to its advantages for industrial applications [25–27]. Using laser treatment, the resin can be separated from the surface without damaging the fibers while there is no need for any mechanical contact and complex fixture systems which provide high flexibility and automation [4].

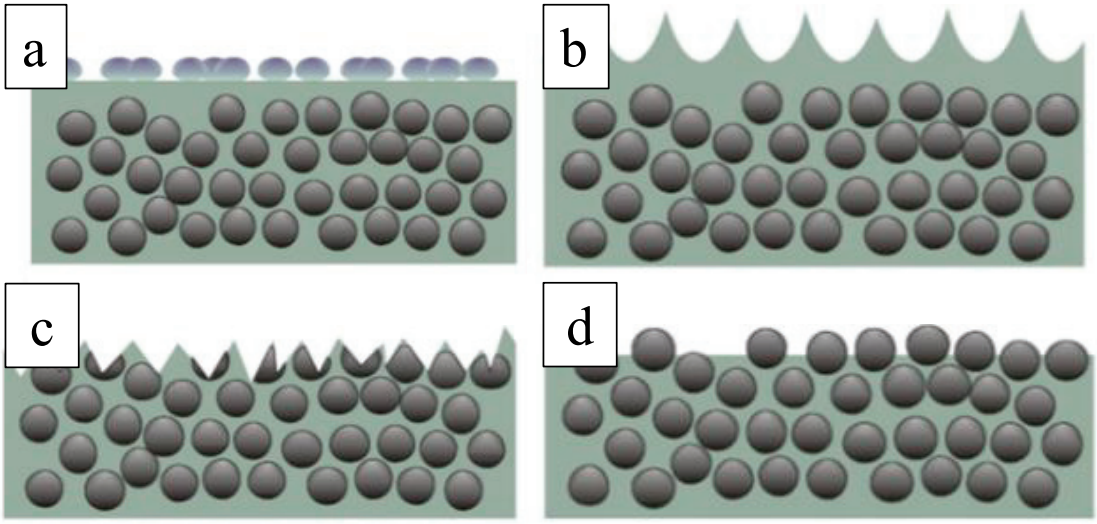

Figure 1. 5. a) Contaminated Surface b) Peel-Ply Surface c) Grinding/Sandblasting Surface d) Matrix Removal Laser Radiation (Source: FISCHER, F., et al., 2012[6]).

1.3.1. Laser Surface Treatment

The laser surface treatment allows selective removal of the polymer matrix over and around the fibers [28](Figure 1.6). During such process, a laser beam applies energy onto surface which heats and irradiates the material, known as laser ablation. The process parameters can be tuned according to irradiation energy limits of different materials forming the composite structure, in order to evaporate only the selected one. The benefits of laser surface treatment of CFRP-laminates for adhesive bonding purposes are three folds. First, the laser surface treatment removes the release agent from the surface. The release agent is an inert substance with negative effects on bonding [23,29]. The second one is polymer matrix on the surface removed and the top layer carbon fiber layers are exposed. Third, the laser surface treatment increases the wettability of the surface [4,30]. As a result, it is possible to obtain a direct attachment to the reinforcement elements and at the same time increase the wettability and remove the contamination on the surface [5,31].

Different kind of laser sources with different wave and pulse lengths have been employed for various objectives [32,33]. The CO_2 lasers were the very first type used to treat the surfaces of polymer matrix composites. Although CO_2 lasers are low cost, there is a

risk of thermal and thermomechanical degradation of the material due to heat accumulation in the material [34–36].

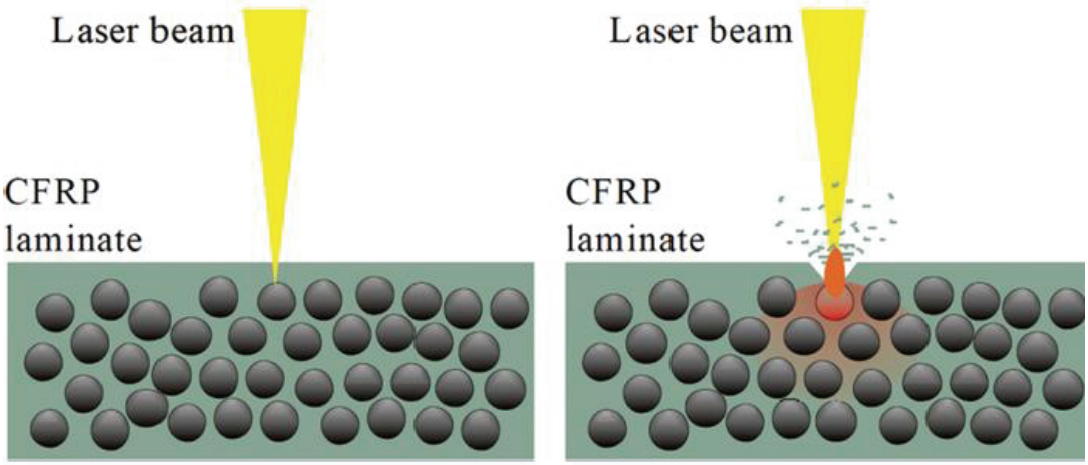

Figure 1. 6. The transmittivity behavior of the (left) matrix material and the (right) absorption of the laser beam on the carbon fibre with the corresponding blast away of the matrix. (Color figure available online.) (Source: FISCHER, F., et al., 2012[6]).

As an alternative, ultra-violet (UV) lasers with shallow laser penetration depth were practiced to remove the layer of matrix and the contaminants without any thermal heating effects by photo-chemical ablation [25,35]. However, UV lasers require high processing time and cost to treat composite surfaces [5]. Instead, processing time and energy use can be substantially decreased by using infrared (IR) lasers [37]. For such a case, it is very important to control the heat affected zone (HAZ) of photo-thermal ablation [10,30,34]. Therefore, there is a big need to determine the optimal laser processing parameters for IR laser application to remove the polymer matrix from the composite surface with low fiber damage and small HAZ extension [5,36](Figure 1.7).

The IR laser range can be guided by an optical fiber which is also well suited for automation. Recent fiber lasers based on master oscillator power amplifier (MOPA) design replaced earlier Q-switched diode-pumped solid-state counterparts. Nowadays, short pulsed fiber lasers are increasingly being used in industry especially for micromachining and advanced surface engineering [35,36]. These type of lasers show unique

advantages in processing anisotropic and inhomogeneous materials such as CFRP, as they are non-contact and wear-free machining tools [6,31].

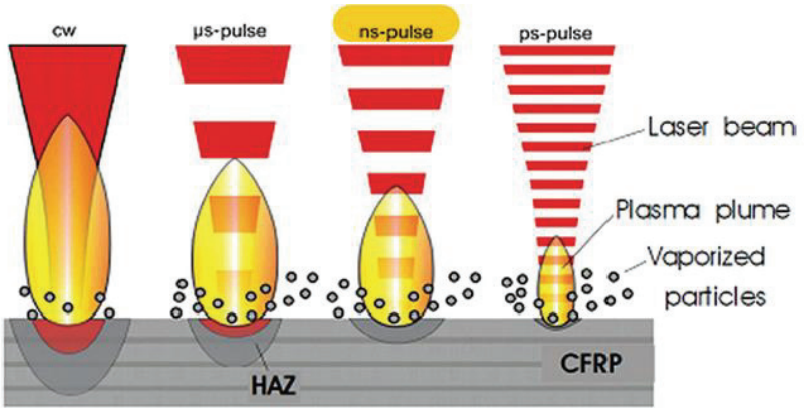

Figure 1. 7. Influence of different pulse durations in comparison to a continuous wave (continuous wave – cw) laser in the laser material ablation. (Source: FISCHER, F., et al., 2012 [6]).

However, use of short-pulsed fiber lasers requires extra attention as the matrix transmits laser energy in the IR range. The measured absorption curves of the epoxy resin showed that the IR laser passes through epoxy resin and reaches the carbon fiber layer directly [38]. Thus, removal of the epoxy from the surface is done by heating the fiber and consequent sublimation of the matrix [17]. Since the CFRP composite materials consist of two different materials with different physical and thermal properties, the mechanism of heat transfer and laser ablation should be carefully tuned by corresponding control parameters.

The laser energy absorbed by the carbon fibers at the interface is converted into thermal energy. Since the thermal properties of carbon fiber and polymer matrix are different, the resin near the interface decomposes and produce gaseous pyrolysis products, while the carbon fibers remain undamaged. With the expansion of the internal pyrolysis gas, the top matrix layer can be removed from the composite surface[7] (Figure 1.8). Therefore, the ablation of matrix material using IR laser is directly related with the heating of the fibers while temperature of fibers should also be under control to keep the HAZ extension low [6]. The energy density value of IR laser is an important parameter in this process. However, application speed becomes equally important in the treatment of

CFRP due to the aforementioned heat transfer mechanisms through the highly conductive fibers. Regardless of its importance, the optimum values of laser energy and application speed yielding a successful epoxy removal with a clean surface, and undamaged fibers are not well correlated in the literature yet.

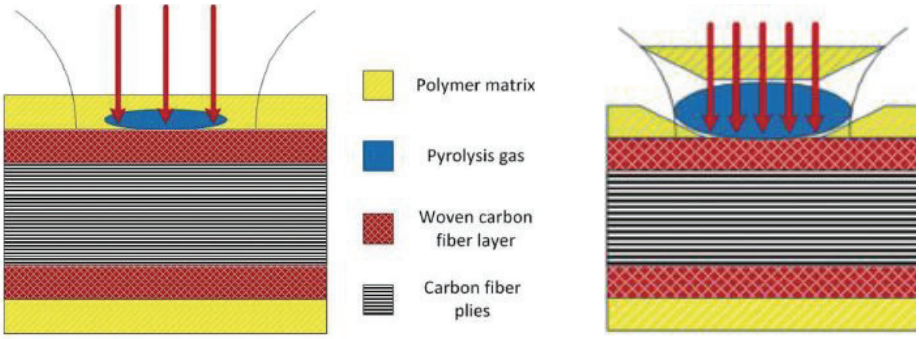

Figure 1. 8. A schematic of pyrolysis gas generated inside of carbon fiber/epoxy composites by 1064nm laser. (Source: LI, Xiao, et al., 2020[5]).

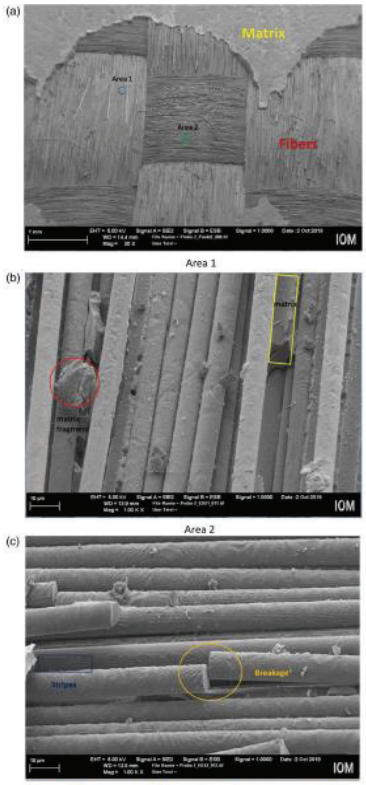

Figure 1. 9. Characteristic morphologies of carbon fibers on the laser-treated composite surface using SEM. (Source: LI, Xiao, et al., 2020[5]).

1.4. Objectives

The aim of this study is to improve the joint area performance of structural fiber reinforced composite parts used in aviation. The purpose of this improvement is to increase the mechanical properties of the connection regions. This study was conducted with an innovative approach to improve joint performance of composites with laser surface modification. In this study, laser surface modification was performed on carbon fiber reinforced polymer plates to improve the performance of the bonding area, and the polymer was selectively removed from the bonding surface. Optical and SEM microscope images were examined and contact angle tests were performed to analyze the laser surface modification. In order to examine how laser surface modification affects the mechanical performance in the bonding zone, reference carbon fiber reinforced composite plates and laser surface modified CFRP composite plates were produced using the hot press method. The prepared plates were cut with wet cutting and lap-shear test, Charpy impact test and DCB test samples were prepared. In addition, lap shear, charpy impact test and DCB tests were repeated after the plates were kept in the environmental chamber to examine the effect of climatic conditions on mechanical properties.

CHAPTER 2

EXPERIMENTAL

2.1. Materials

CFRP composite laminates fabricated with (UD) unidirectional, with a unit weight of 294 g / m^2, $[45/0/-45/90]_{2s}$ stacking sequence of 16 layers of carbon/epoxy prepregs (Carbon Epoxy. M91 / 34 / UD194 / IM7-12K) were used. The prepregs used were chosen for use in aerospace primary structures with a high performance and very tough epoxy matrix. The composite laminates were fabricated by stacking under vacuum followed by a curing stage performed at 180 °C, and 7 bar for 2 hours with autoclave technique. Finally, 3 mm thick plates with a final size of 30 cm × 30 cm were manufactured. The CFRP lamination lay-up is schematically illustrated in Figure 2.1.

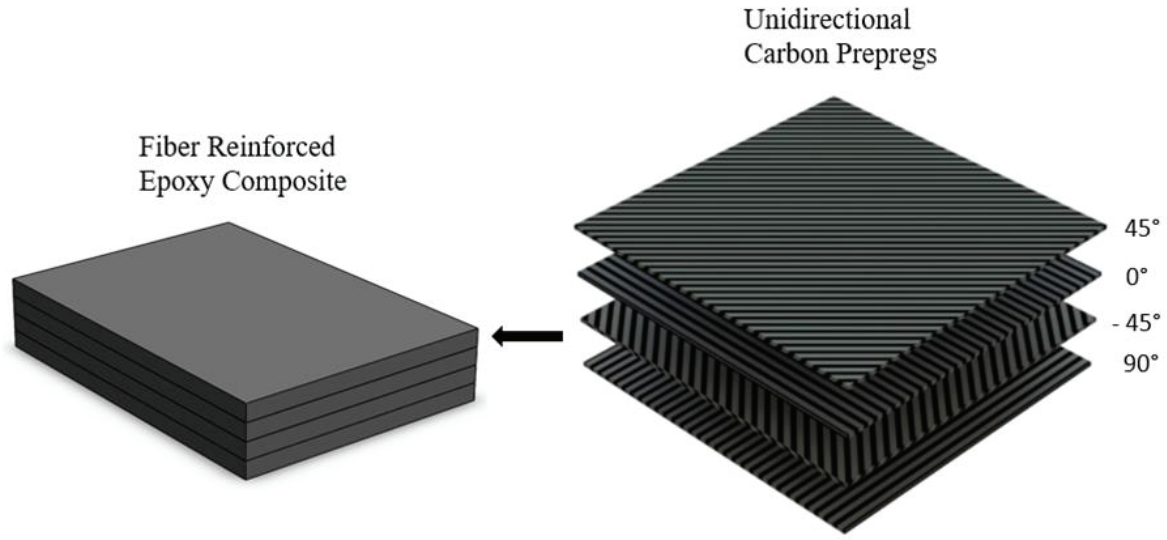

Figure 2. 1. The illustration of CFRP panel development by stacking the 16 layers of unidirectional carbon/epoxy prepregs (HexPly® M91) in $[45/0/-45/90]_{2s}$ sequence.

2.2. Preparation of CFRP Plate Surface

The laser treatment was carried out using an IR-Yb (Ytterbium) fiber nanosecond laser (FLAST-NanoMARK-50w) with the following parameters: wavelength of 1064 nm, frequency of 100 kHz, spot diameter 30 nm and pulse width of 100 ns. The laser system is shown in Figure 2.2a. Laser average power, frequency and speed are the parameters of the energy applied by the laser spot onto the surface. The lowest power that can remove the epoxy from the surface, the highest scanning speed of the device and the lowest frequency were selected. The power is 20 W, the speed is 10000 mm/s and the frequency is 100 kHz. Experiments were carried out using 3 different laser offset distances of 0.15, 0.20 and 0.25 mm to remove the epoxy from the surface and observe the best adhesion performance.

A square shape application area was defined in accordance with the fiber direction of the fabric in line with laser treatment. Laser was applied on surface with single scanning as shown in Figure 2.2b.

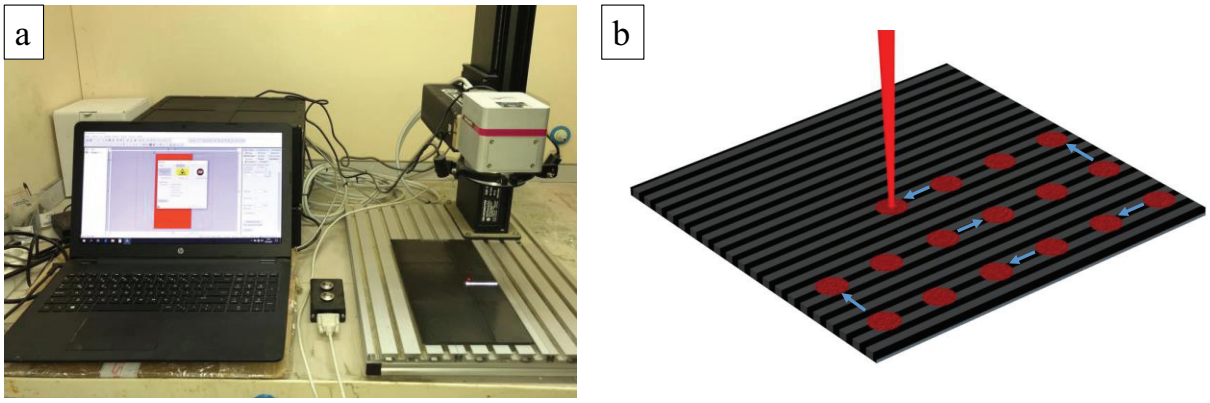

Figure 2. 2. (a) The fiber laser system and (b) laser spot distribution diagram.

The energy density (ED) of each laser pulse as a function of varying laser power (P) and the laser scanning speed (V_{scan}) was obtained as below,

$$ED = \frac{P}{V_{scan}\ x\ D_{spot}} \quad (1)$$

As shown in Table 2.1, the laser offset distance was varied to determine the optimum laser ablation parameters. W (laser average power) and V_{scan} (laser scanning speed) and f (frequency) parameters were kept constant.

Table 2. 1. Relationship between laser avg. power (W) and laser energy density (ED).

Laser Parameters	**A**	**B**	**C**
Laser Offset Distance (mm)	0.15	0.20	0.25
Avg. Power (W)	20	20	20
Scanning Speed (mm/s)	10000	10000	10000
Laser Diameter (µm)	30	30	30
Energy Density (mJ/mm^2)	66.67	66.67	66.67
Number of Repetitions	1	1	1
Frequency (kHz)	100	100	100

2.3. Contact Angle Analysis

Contact angle tests were performed with KSV Attension brand, Theta model contact angle and surface tension device (Figure 2.3.) in our department's laboratory. In order to determine the laser ablation efficiency and to see the change in roughness, contact angle tests were performed on three different points of the laser ablated surface.

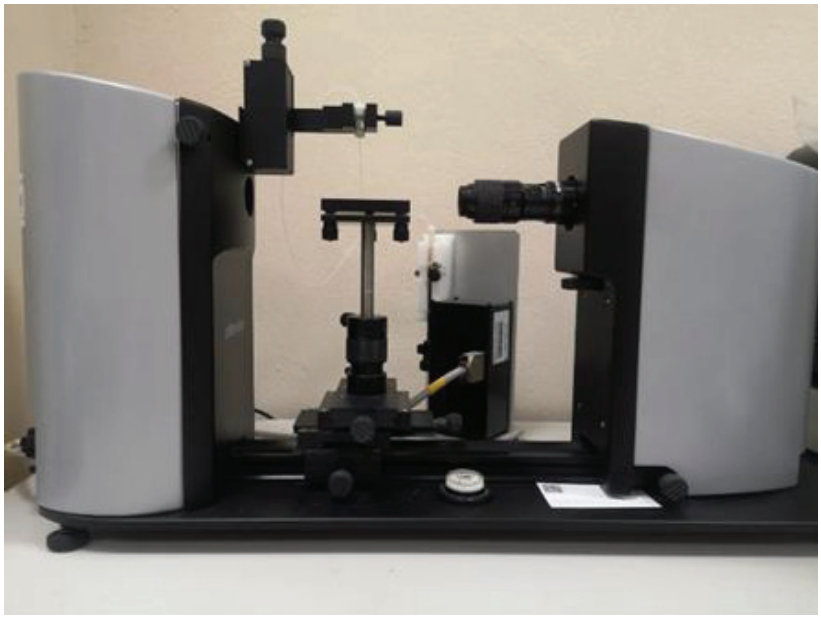

Figure 2. 3. Contact angle and surface tension device in our laboratory.

The effect of laser offset distances on the wettability behavior is shown in Table 2.2. According to the contact angle results, sample A with laser surface modification with a laser offset distance of 0.15 mm showed the lowest contact angle, thus the best wettability behavior, while the reference sample showed the highest contact angle and thus the worst wettability behavior. According to the contact angle results, the B sample with laser surface modification with a laser offset distance of 0.20 mm showed a low contact angle, thus a good wettability behavior, while the C sample with a laser surface modification with a laser offset distance of 0.25 mm showed a high contact angle and a bad wettability behavior. The effect of laser offset distance on wettability behavior was supported by contact angle tests.

Table 2. 2. Contact angle results for samples REF, A, B and C

Sample	Time (s)	Contac Angle (°)
REF	0	66.051
	60	63.351
A	0	53.681
	60	49.991
B	0	53.904
	60	50.214
C	0	60.114
	60	56.916

Figure 2.4 shows the contact angle test photographs of reference sample, sample A (laser treated with 0.15 mm offset distance), sample B (laser treated with 0.20 mm offset distance), and sample C (laser treated with 0.20 mm offset distance). Figure a1, a2 and a3 shows the contact angle test photographs of the reference sample at the 1st, 30th and 60th seconds. Figure b1, b2 and b3 show the contact angle test photographs of the A sample at the 1st, 30th and 60th seconds. Figure c1, c2 and c3 show the contact angle test photographs of sample B at 1, 30 and 60 seconds. Figure d1, d2 and d3 shows the contact angle test photographs of sample C at 1, 30 and 60 seconds. Laser surface modification increased the roughness on the surface, resulting in a more hydrophilic surface. The more the droplet spreads on the surface, the greater the hydrophilicity, hence the wettability. It was observed that the water droplet in the A sample spread slightly more than the water droplets in the REF, B and C samples, so the wettability properties were higher. Thus, laser ablation effects could be observed visually.

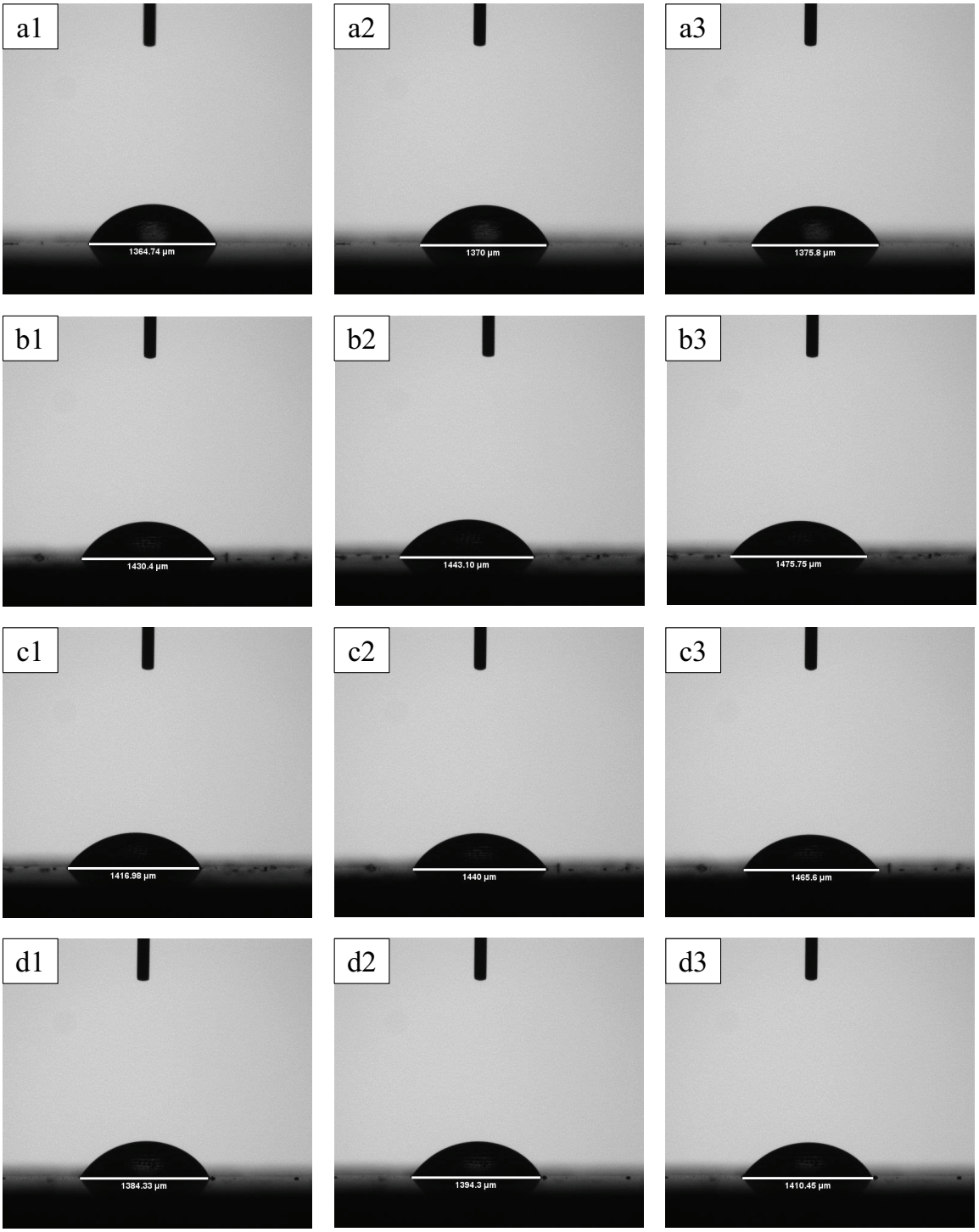

Figure 2. 4. Contact angle results a) REF(Reference), b) Sample A, c) Sample B and d) Sample C, 1) 1st second, 2) 30th second, and 3) 60th second

2.4. Optical Microscope Images

In Figure 2.5, optical microscope images of samples A, B and C are shown. Figure 2.5a shows the 0.15 mm laser offset distance, Figure 2.5b shows the 0.20 mm laser offset distance, Figure 2.5c shows optical images of the 0.25 mm laser offset distance. It is observed that the laser pulses at the selected power, speed and frequency completely remove the epoxy and the fibers are visible.

Figure 2. 5. Optical microscope images for samples with different laser offset distance a) 0.15 mm, b) 0.20 mm and c) 0.25 mm.

2.5. SEM Images

SEM images of the samples whose parameters are given in Table 2.1 were taken, and the epoxy residues and fibers seen in the optical microscope image were examined in detail. In Figure 2.6, the SEM image of the non-laser scanned surface is shown as a reference.

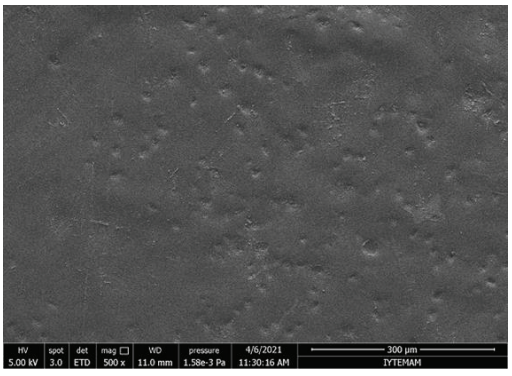

Figure 2. 6. SEM image of reference sample.

In Figure 2.7, SEM images of the plates with laser surface modification with 0.15 mm laser offset distance are shown at different magnifications. It is observed that the epoxy on the surface is removed with laser pulses, but some fibers are also damaged. For this reason, the energy applied to the surface by the 0.15 mm laser offset distance is high.

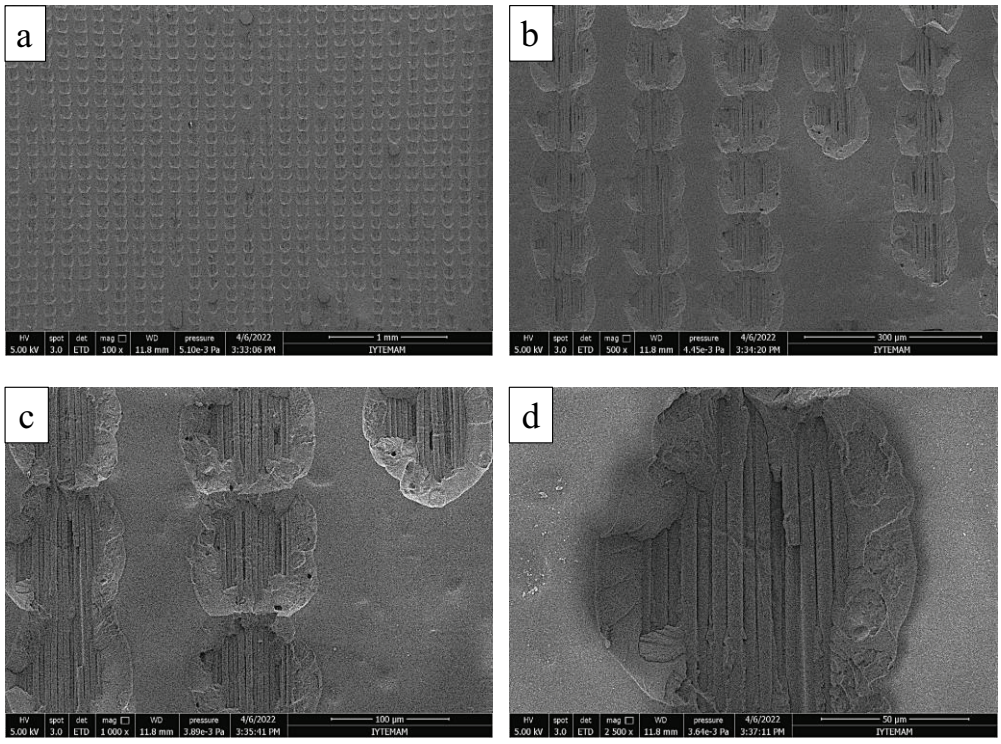

Figure 2. 7. SEM images of the sample with 0.15 mm laser offset distance.

In Figure 2.8, SEM images of the plates with laser surface modification with a laser offset distance of 0.20 mm are shown at different magnifications. It is observed that the epoxy on the surface is removed with laser pulses and the fibers are not damaged. For this reason, the energy applied by the 0.20 mm laser offset distance to the surface is sufficient to remove the epoxy and is also suitable for not damaging the fibers.

In Figure 2.9, SEM images of the laser surface modified plates with a laser offset distance of 0.25 mm are shown at different magnifications. It was observed that the epoxy on the surface could not be removed at some points with laser pulses. For this reason, the energy applied by the 0.25 mm laser offset distance to the surface is not enough to remove the epoxy clearly.

It was aimed to remove the epoxy from the surface without damaging the fibers, and the epoxy was successfully removed from the surface.

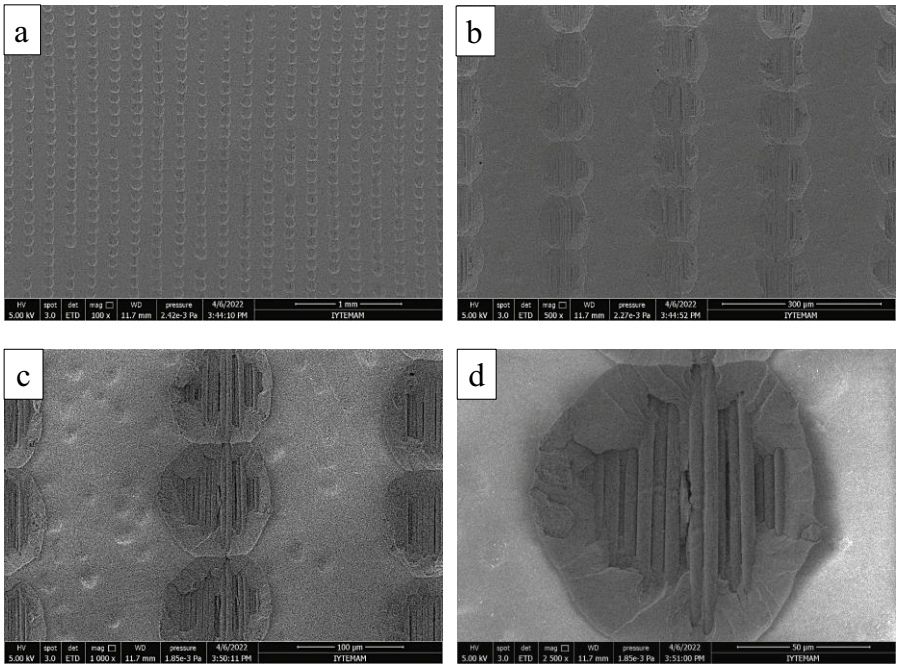

Figure 2. 8. SEM images of the sample with 0.20 mm laser offset distance.

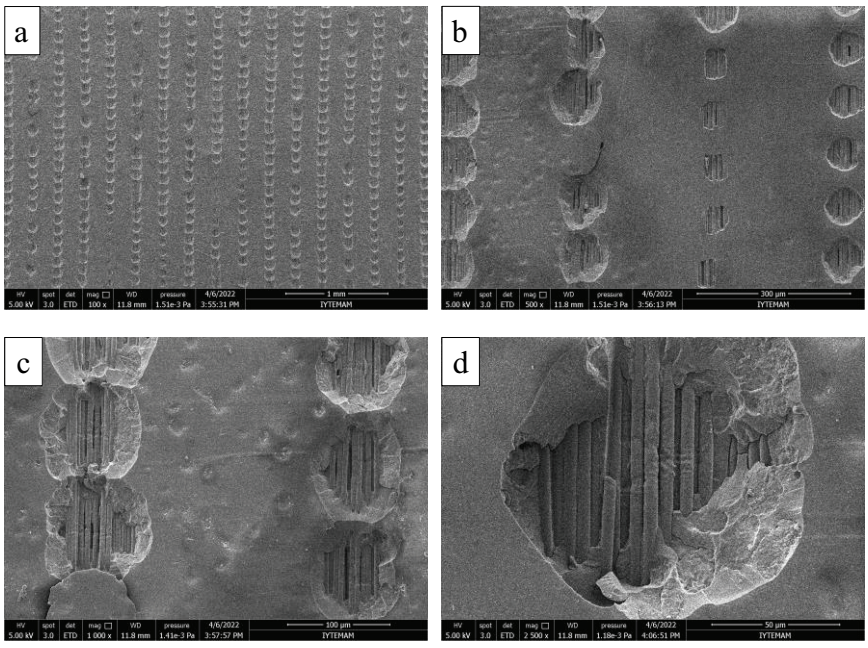

Figure 2. 9. SEM images of the sample with 0.25 laser offset distance.

2.6. Secondary Bonding Joining of Laser Surface Treated Plates for Mechanical Tests by Hot Press Method

Test specimens were produced for lap shear, charpy impact and DCB tests with reference to ASTM D5868, ISO 179, ASTM D5528 standards, from UD prepreg plates treated with laser surface modification method. 4-layer film adhesive (FM300K) was used as the adhesive material (figure 2.10b).

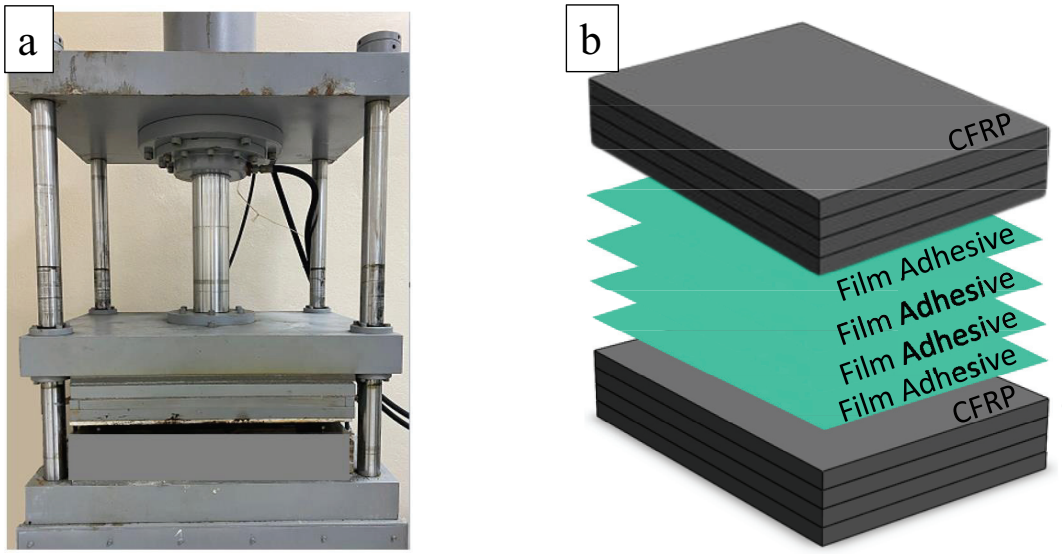

Figure 2. 10. a) Hot Press b) Composite plate to be produced secondary bonding with Hot Press method

Composite plate produced from UD composite prepreg is used as the adherent material (Table 2.3). The prepared composite plates were left to cure in the hot press device in our laboratory at 180 °C and 5 bar pressure for 2 hours (Figure 2.10a). The produced composites were cut by the standards with a wet saw cutting device. The test specimens cut in the wet cutting device were left to dry for 1 hour at 50 °C. The average thickness of the composite samples was measured as 5.80 mm.

Table 2. 3. Test sample production conditions.

Laminate Type	Adhesive Type	Bondline Thickness (mm)	Test Temperature
UD	Film	0.80 (4plies)	RTD

2.7. Single Lap Shear Test

In order to determine shear strength, all single lap shear tests were performed according to ASTM 5868-01 standards. The lap joint tester is shown in Figure 2.11. MTS Landmark™ Servohydraulic Test System was used. The load applied during the test was applied at a speed of 13 mm/min according to the ASTM D5868-01 standard.

Figure 2. 11. Test set-up for the single-lap joint.

4 layers of FM300K film adhesive cut in the same size were placed between the UD prepreg plates whose joint location was laser ablated. It was left to cure for 120 minutes under 5 bar pressure in the Hot press device, which was previously set at 180 °C. The assembled plates were cut in a wet cutting device in accordance with ASTM D5868 test standards and left to dry for 1 hour at 50 °C. Prepared test coupons are shown in Figure 2.12. Five samples were tested for each group to obtain consistent mean and standard deviation values.

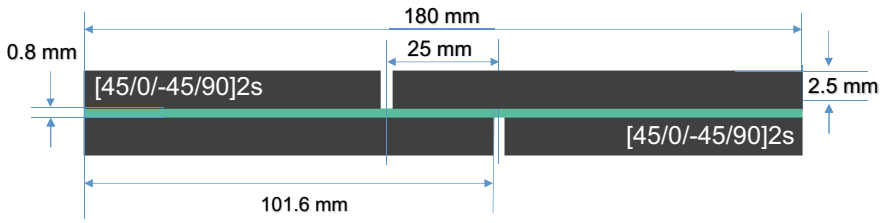

Figure 2. 12. Lap Shear test specimen joined by the secondary bonding method.

2.8. Charpy Impact Test

CEAST® Resil Impactor with a maximum energy of 15 J - 25 J and a tangential speed of 3.46 m/s was used for Charpy impact tests. The samples were produced in accordance with the ISO-179 standard, by cutting 10 x 80 mm rectangles and then notching 2 mm. Charpy impact energy is calculated by dividing the impact energy by the notched area. Eight samples were tested for each group to obtain consistent mean and standard deviation values. Prepared test coupons are shown in Figure 2.14.

Figure 2. 13. Test set-up for the charpy impact test.

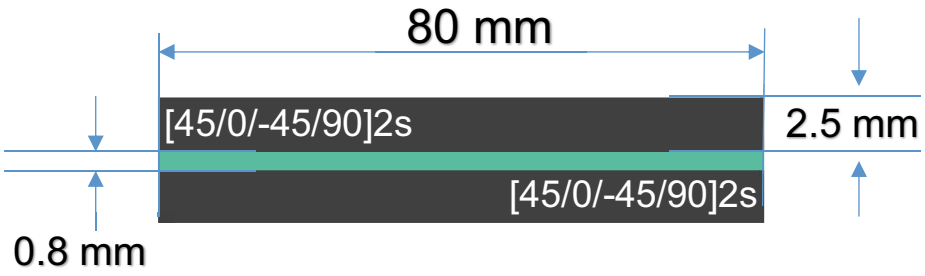

Figure 2. 14. Charpy impact test specimen joined by the secondary bonding method.

2.9. Double Cantilever Beam Tests

Double cantilever beam (DCB) test was applied to obtain the Mode-I laminar fracture toughness (G_{IC}) of the CFRP material. The name and model of the device used is Shimadzu AGS-X, Kyoto, Japan, test device with 5 kN load cell, as shown in Figure 2.15. The samples were prepared according to the ASTM5528-13 standard, schematically as shown in figure 2.16.

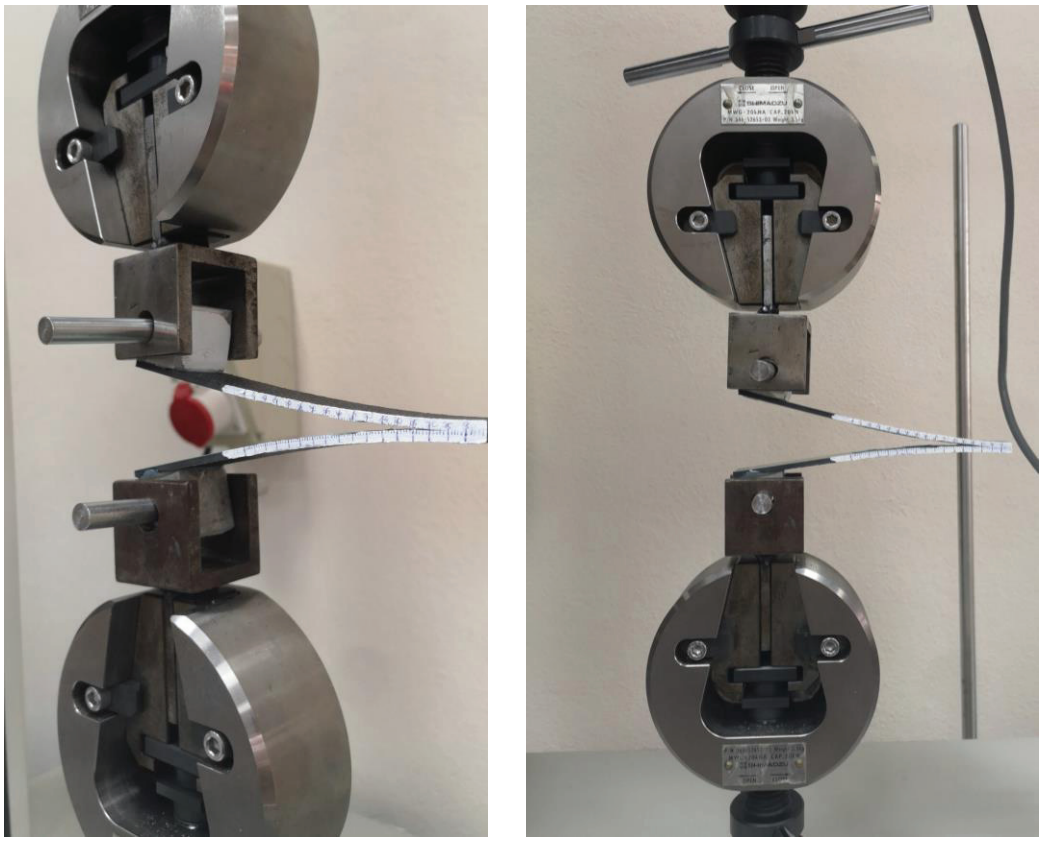

Figure 2. 15. Test set-up for the DCB.

DCB specimens were cut with a wet cutting device at 150 mm (L) length and 25.4 mm (b) width after the plates were bonded with secondary bonding. Then, 25mm cubes were attached to the samples. Then, after the side section was painted white, a ruler was drawn with a gap of 1 mm. Cubes use it to transmit force to the sample. It is used to observe crack progression with the ruler image.

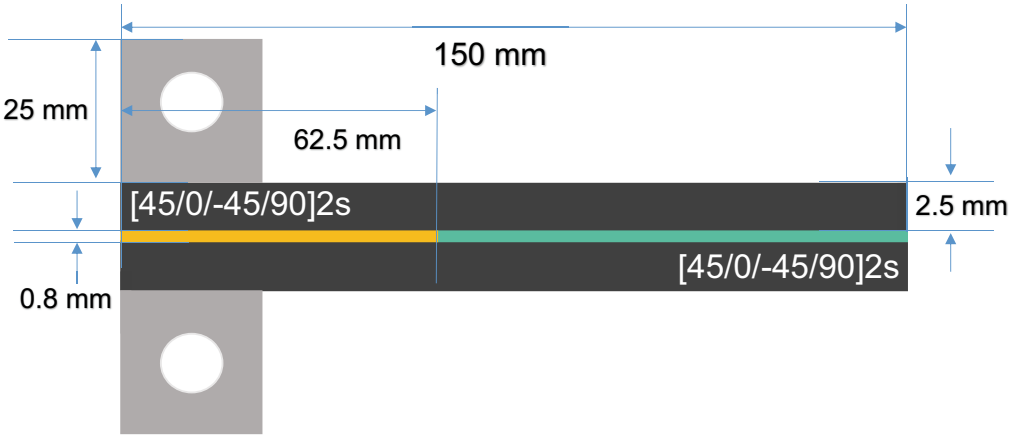

Figure 2. 16. DCB test specimen joined by the secondary bonding method.

The DCB test steps can be explained as follows, the samples were loaded at a speed of 1 mm/min for the first crack to form and advance 3-5 mm. The final load continued to be loaded until the crack advanced 70 mm. During the test, the load, crack propagation length and displacement values were recorded to calculate fracture toughness. By visually observing the initial G_{IC} (G_{ICini}) value from the criterion drawn on the fractured surface of the sample, the G_{IC} value of the delamination was computed. The crack propagation and G_{IC} values were averaged to provide the G_{IC} spread (G_{ICprop}) value. The Modified Beam Theory reduction method was used to calculate the values of G_I, G_{ICini}, and G_{ICprop} [39].

For energy release rate (G_I) analysis, the load of the sample, crack opening displacement, and fracture length were recorded during the testing. The G_I was calculated using the conventional data reduction technique described below [39].

$$G_I = \frac{3P\delta}{2b(\alpha + |\Delta|)} \quad (2)$$

Mode-I interlayer fracture toughness is the G_I in the equation. A load, specimen width, delamination length, and load point displacement are all called as *P, b,* α*,* and δ , respectively. The Δ value is determined experimentally by building a least-squares plot of the root of feet ($C^{1/3}$) as a crack length equation. The error parameters F and N are utilized to compute the displacement and specimen hardening. F takes into account the moment arm's shortening and the end blocks' bending. N takes into account the blocks' ability to harden the sample. Below are some correction factor equations [39];

$$F = 1-(\frac{3}{10})(\frac{\delta}{\alpha})^2 - (\frac{3}{2})(\frac{\delta t}{\alpha^2}) \quad (3)$$

$$N = 1-(\frac{L'}{\alpha})^3 -(\frac{9}{8})\left[1 - \left(\frac{L'}{\alpha}\right)^2\right]\left(\frac{\delta t}{\alpha^2}\right) - \frac{9}{35}(\frac{\delta}{\alpha})^2 \quad (4)$$

Figure 2.17 shows the t and L' values in the samples. Based on measurements plotted at one edge of the sample, the initial G_{IC} ($G_{IC,ini}$) data were derived as G_{IC} data in which crack propagation was seen. Analysing G_{IC} spread ($G_{IC,prop}$) data involved averaging the G_{IC} values throughout the delamination process. The behavior of a composite test specimen under Mode-I loading is depicted in Figure 2.17.

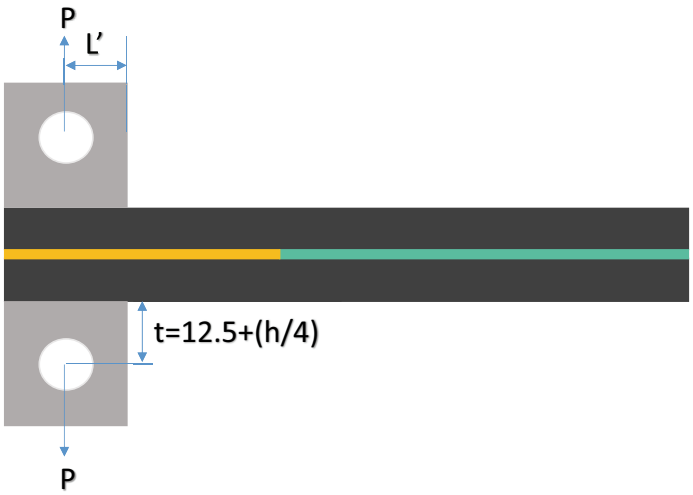

Figure 2. 17. Dimensional relationship between the DCB test specimen and the aluminium blocks adhered to it to transfer the opening forces

2.10. Environmental Aging

The effects of environmental aging on the adhesion performance of unidirectional fiber / epoxy composite materials on the joint area were investigated to simulate the exposed humidity and temperature conditions. For three different types of tests (lap shear, charpy impact and DCB), UD composite plates bonded with film adhesive using the hot press method were exposed to the aging cycle. The Angelantoni DY 340 C computer controlled environmental chamber shown in Figure 2.18 was used for aging cycle. Aging cycle was determined based on the conditions that the aircraft could be exposed to in operating conditions. To simulate the aircraft's moisture intake during flight, the plates were exposed to 70°C, 85% relative humidity for 1.5 months. Then, the lap shear, charpy impact and DCB test samples were prepared with the wet cutting device as ASTM D5868, ISO 179, ASTM D5528 standards.

Figure 2. 18. Photo of environmental chamber

2.11. Moisture Absorption Test

Moisture uptake records were taken after environmental aging to investigate the moisture absorption rate during aging cycle. CFRP composite plates of before and after environmental aging were weighed and recorded. Measurements were taken at the end of cycles to prevent undesired thermal shocks that can occur.

The weight of the CFRP bonded composite plate before aging is 220.84 gr. Figure 2.19 shows the weight of the CFRP bonded composite plate after the aging cycle. The weight of the CFRP bonded composite plate after aging is 230.96 g. Changes in the weight of the CFRP bonded plate were observed as a function of humidity with the aging cycle. The moisture content of the unidirectional composite plate sample increased by only 10.12 grams at the end of the aging cycles, corresponding to a 4.58% mass gain due to moisture uptake.

Figure 2. 19. Photo of sample weight after aging

CHAPTER 3

RESULTS AND DISCUSSION

3.1. Single Lap Shear Test

Shear strength properties of composite specimens whose joint location was modified by laser ablation were investigated. Single lap shear tests were performed with ASTM D5868. Samples were prepared to evaluate the adhesion strength of UD prepreg plates adhered with FM300K film adhesive. Laser ablation was performed on the adhesion surfaces of the plates with 3 different laser offset distances. Optimum parameters of the study were determined by choosing the parameter that provides the best increase among these 3 different laser offset distances.

Pre- and post-test images of the reference samples are shown in Figure 3.1. Results are calculated based on the cross-sectional area of the test specimens.

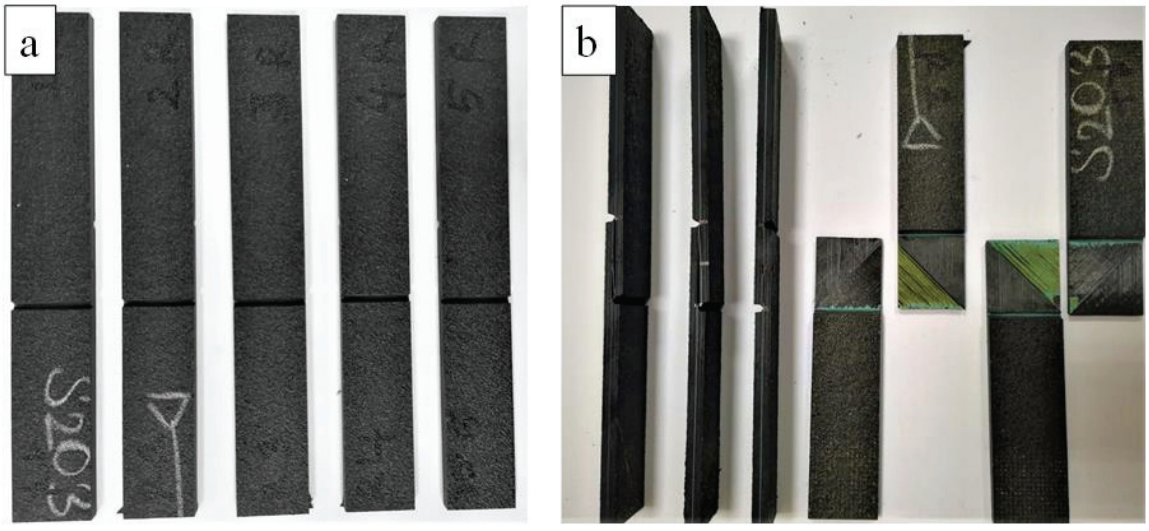

Figure 3. 1. Single lap shear reference test specimen produced with the secondary bonding method a) Before the test b) After the test (the fracture surface)

The pre-test and post-test images of the laser surface modified samples with 0.15 mm laser offset distance are shown in Figure 3.2. Results were calculated based on the cross-sectional area of the test specimens.

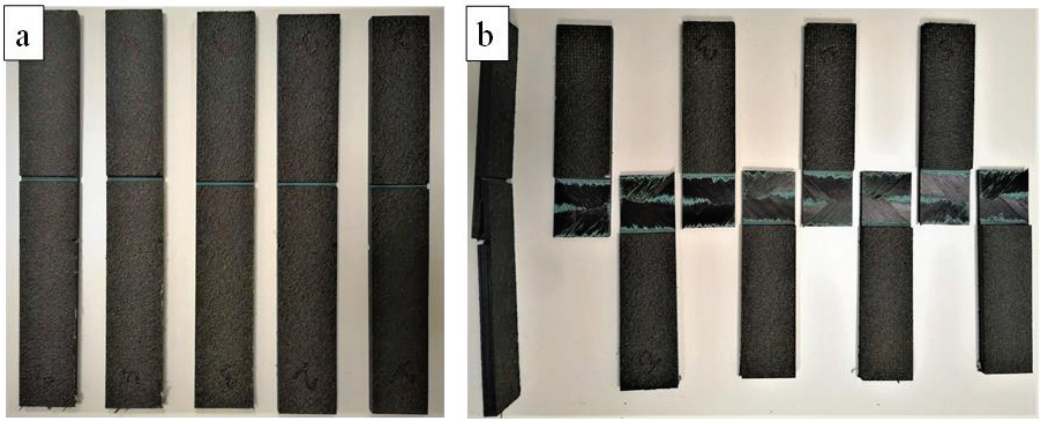

Figure 3. 2. Single lap shear test specimen A (laser surface modification with 0.15 mm laser offset distance) a) Before the test b) After the test (the fracture surface)

The pre-test and post-test images of the samples with laser surface modification at 0.20 mm laser offset distance are shown in Figure 3.3. Single lap shear test results were calculated based on the cross-sectional area of the test specimens.

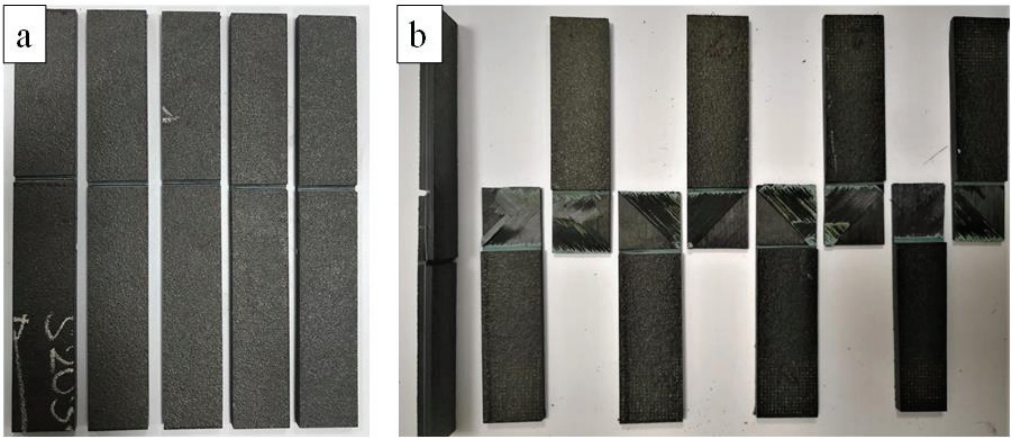

Figure 3. 3. Single lap shear test specimen B (laser surface modification with 0.20 mm laser offset distance) a) Before the test b) After the test (the fracture surface)

The pre-test and post-test images of the samples with laser surface modification at 0.25 mm laser offset distance are shown in Figure 3.4. Results are calculated based on the cross-sectional area of the test specimens.

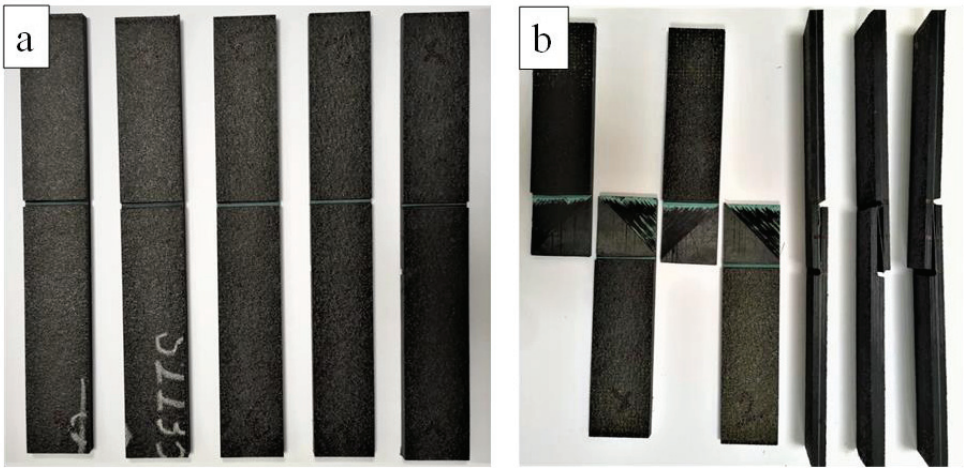

Figure 3. 4. Single lap shear test specimen C (laser surface modification with 0.25 mm laser offset distance) a) Before the test b) After the test (the fracture surface)

When the fracture surfaces of the joint area were examined, it was observed that the laser modified samples adhered to the adhesive better than the reference samples. While the adhesive was more visible in the reference samples, the visibility of the adhesive decreased, and the fiber visibility increased in the laser samples. In the samples modified with laser, the film adhesive penetrated more fibers and increased the adhesion.

Table 3.1 shows the lap shear test results of laser ablated composite specimens with reference and 3 different laser offset distances. The average shear strength of the reference composite samples in Table 3.1 is 17.44 MPa. The average shear strength of the 0.15 mm offset distance laser ablated samples decreased compared to the reference samples and was 16.92 MPa. The average shear strength of the laser ablated samples with 0.20 mm laser offset distance showed an improvement of 13.87% compared to the reference samples and was 19.46 MPa. The average shear strength of the laser ablated samples with 0.25 mm laser offset distance showed an improvement of 7.59% compared to the reference sample and was 18.39 MPa. When the test results in Table 3.1 are

examined, the highest increase in shear strength was observed in the samples with 0.20 mm laser offset distance. The laser surface modification process has proven to show a significant increase in shear strength. Laser surface modification is a good method to reduce joint area fragility.

Table 3. 1. Lap Shear Test Results

Sample	Shear Strength (MPa)			
	Reference	A (0.15 mm Laser Offset Distance)	B (0.2 mm Laser Offset Distance)	C (0.25 mm Laser Offset Distance)
1	16.71	17.77	19.07	19.04
2	16.37	15.92	19.16	17.44
3	17.00	17.47	19.77	17.78
4	17.73	16.06	19.44	18.94
5	17.64	17.36	19.86	18.73
Avarage	17.09	16.92	19.46	18.39
Standard Deviation	0.59	0.86	0.35	0.73
Improvement (%)	-	-1.01	13.87	7.59

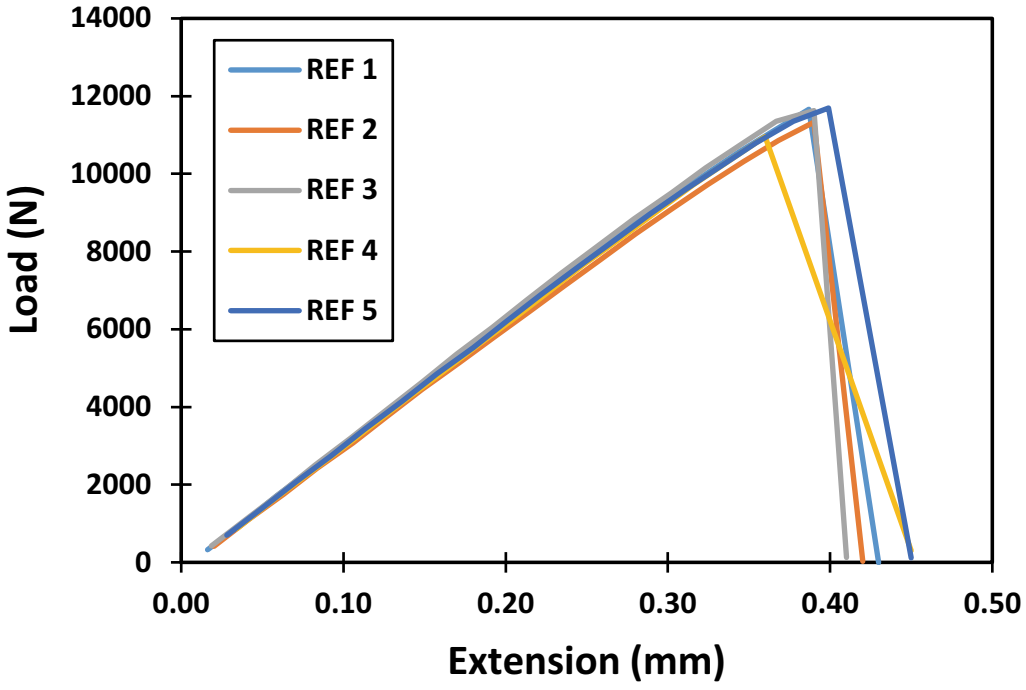

Figure 3. 5. Load vs. extension curves of reference specimens according to single lap shear test.

Shear load-extension diagrams of reference samples are shown in Figure 3.5. Single lap shear test results were calculated based on the force-displacement curve and the cross-sectional area of the test specimens.

Shear load-extension diagrams of samples laser treated with 0.15 mm laser offset distance are shown in Figure 3.6. Single lap shear test results were calculated based on the force-displacement curve and the cross-sectional area of the test specimens.

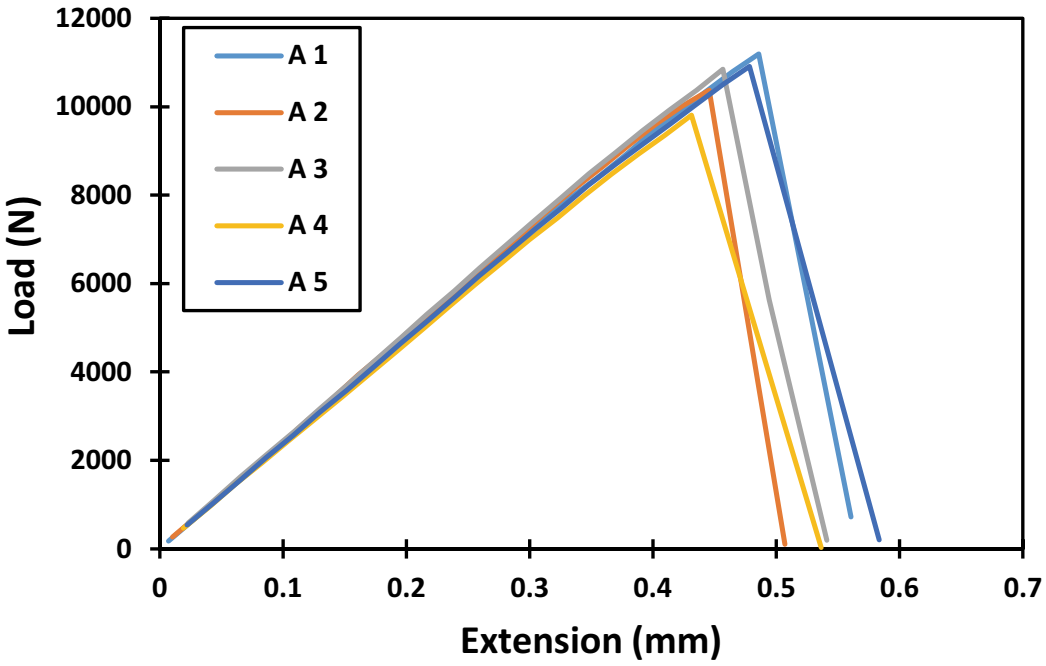

Figure 3. 6. Load vs. extension curves of laser surface treated with 0.15 mm laser offset distance specimens according to single lap shear test.

Shear load-extension diagrams of samples laser treated with 0.20 mm laser offset distance are shown in Figure 3.7. Single lap shear test results were calculated based on the force-displacement curve and the cross-sectional area of the test specimens.

Shear load-extension diagrams of samples laser treated with 0.25 mm laser offset distance are shown in Figure 3.8. Single lap shear test results were calculated based on the force-displacement curve and the cross-sectional area of the test specimens.

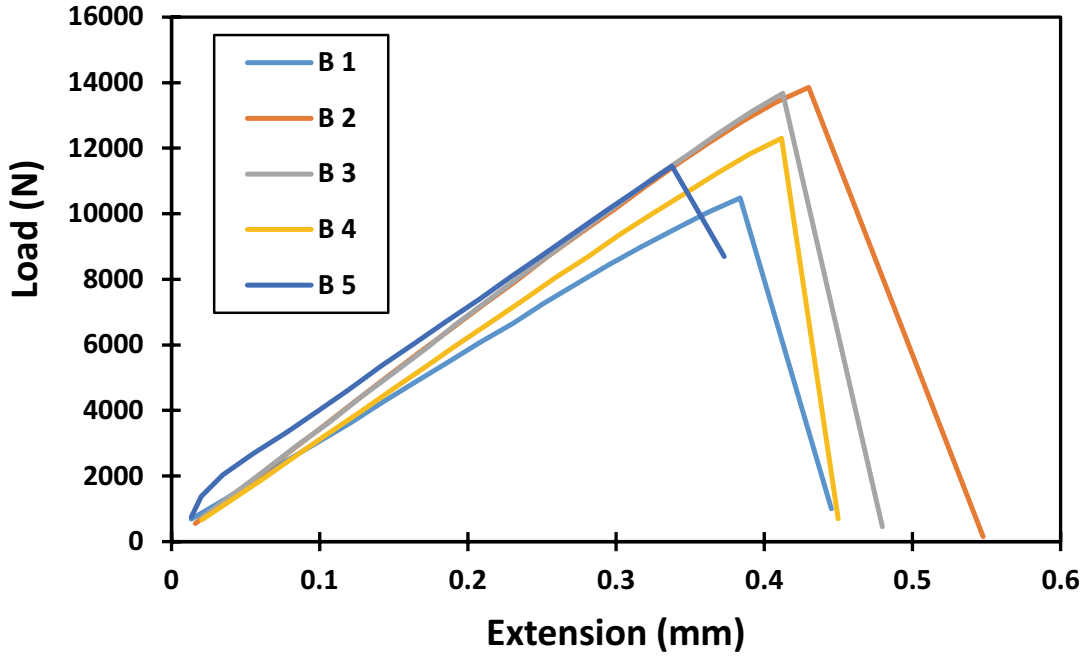

Figure 3. 7. Load vs. extension curves of laser surface treated with 0.20 mm laser offset distance specimens according to single lap shear test.

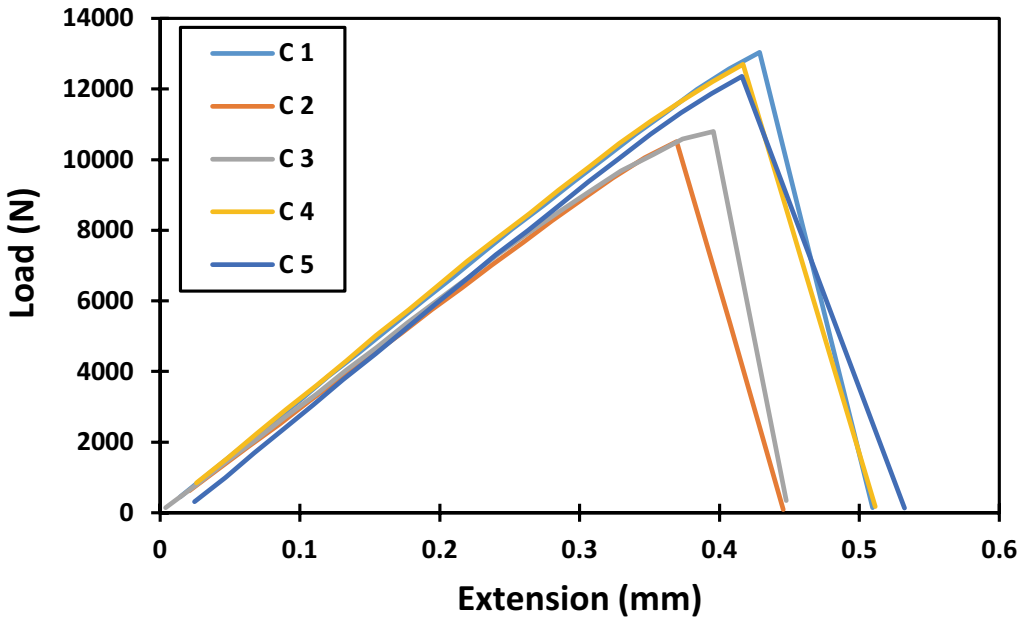

Figure 3. 8. Load vs. extension curves of laser surface treated with 0.25 mm laser offset distance specimens according to single lap shear test.

Figure 3.9 and Figure 3.10 show the fracture surfaces and SEM images of the reference and laser surface modified composites' fracture surface, after the lap shear test. When the fracture surfaces of the joint area were examined, it was observed that the laser-modified samples adhered better. When the joint area of the reference sample was examined, it was observed that the fracture mode was adhesive failure. When the joint area of the composite sample, which was laser modified with a laser offset distance of 0.15 mm, was examined, it was observed that the fibers were damaged and broken from the fiber due to high laser energy. When the joint region of the composite sample, which laser surface modification with a laser offset distance of 0.20 mm, was examined, it was observed that the fracture mode was fiber-tier failure. In these samples, it was determined that the adhesive increased the bond strength by penetrating more fibers. When the joint area of the composite sample, which laser surface modification with a laser offset distance of 0.25 mm, was examined, it was observed that the fracture mode was light-tear failure. In these samples, it was observed that the adhesive penetrated the fibers more than the reference but less than the samples with 0.20 mm laser offset distance. Examining the test results, it was proved that the laser surface modification treatment showed a significant increase in bonding strength. Laser surface modification is a good method to reduce joint area fragility.

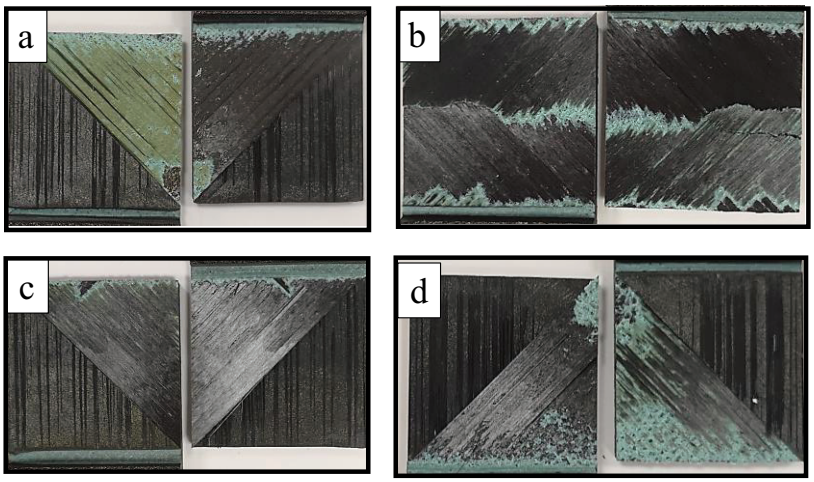

Figure 3. 9. The fracture surface of a) reference samples, b) laser treated with 0.15 mm offset distance samples, c) laser treated with 0.20 mm offset distance samples, d) laser treated with 0.25 mm offset distance samples after single lap shear test.

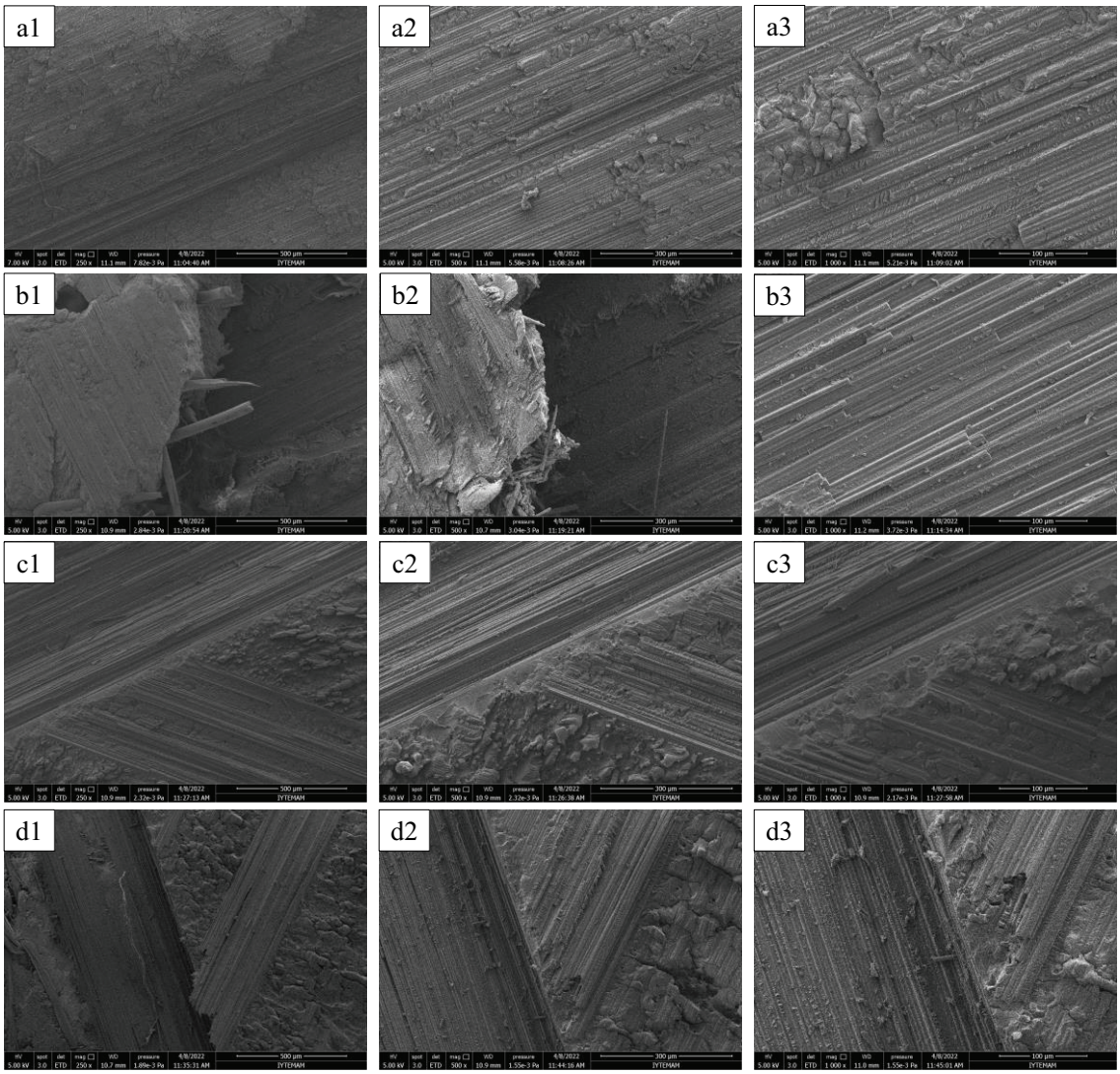

Figure 3. 10. Shows the fracture surface SEM images of the a) reference samples, b) laser treated with 0.15 mm offset distance samples, c) laser treated with 0.20 mm offset distance samples, d) laser treated with 0.25 mm offset distance samples after single lap shear test at different magnification 1) 250x, 2) 500x, and 3) 1000x

3.2. Charpy Impact Test Results

The charpy impact energy properties of composite specimens whose joint area was modified by laser ablation were investigated. Charpy impact tests were carried out with the ISO-179 standard. Samples were prepared to evaluate the adhesion strength of UD prepreg plates adhered with FM300K film adhesive. Laser ablation was performed

on the adhesion surfaces of the plates with 3 different laser offset distances. Optimum parameters of the study were determined by choosing the parameter that provides the best increase among these 3 different laser offset distances.

The images of the reference samples before and after the charpy impact test are shown in Figure 3.11. Results are calculated based on the cross-sectional area of the test specimens.

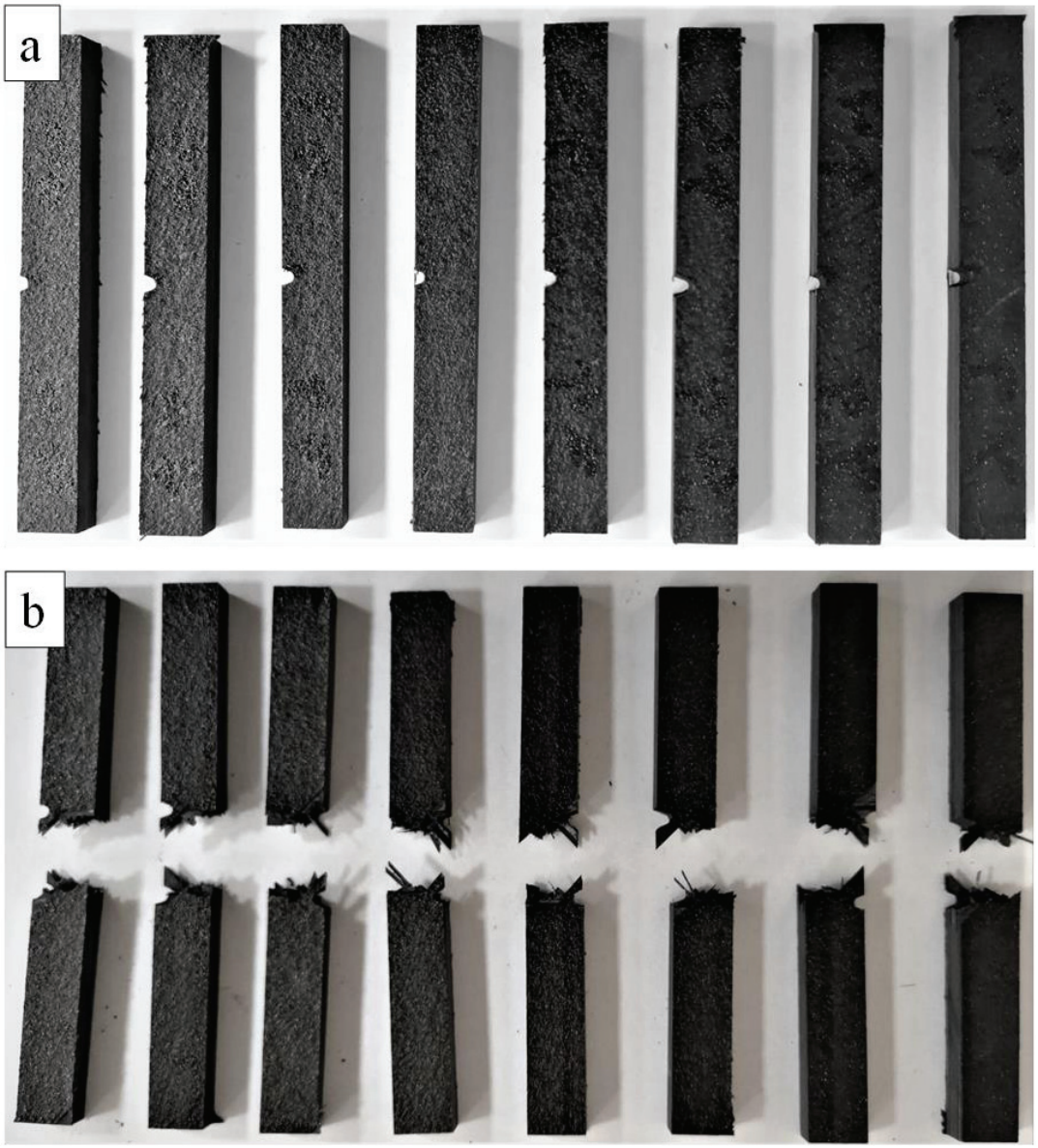

Figure 3. 11. Charpy impact test reference specimen produced with the secondary bonding method a) Before the test b) After the test

The pre-test and post-test images of the laser surface modified samples with 0.15 mm laser offset distance are shown in Figure 3.12. Single lap shear test results were calculated based on the cross-sectional area of the test specimens.

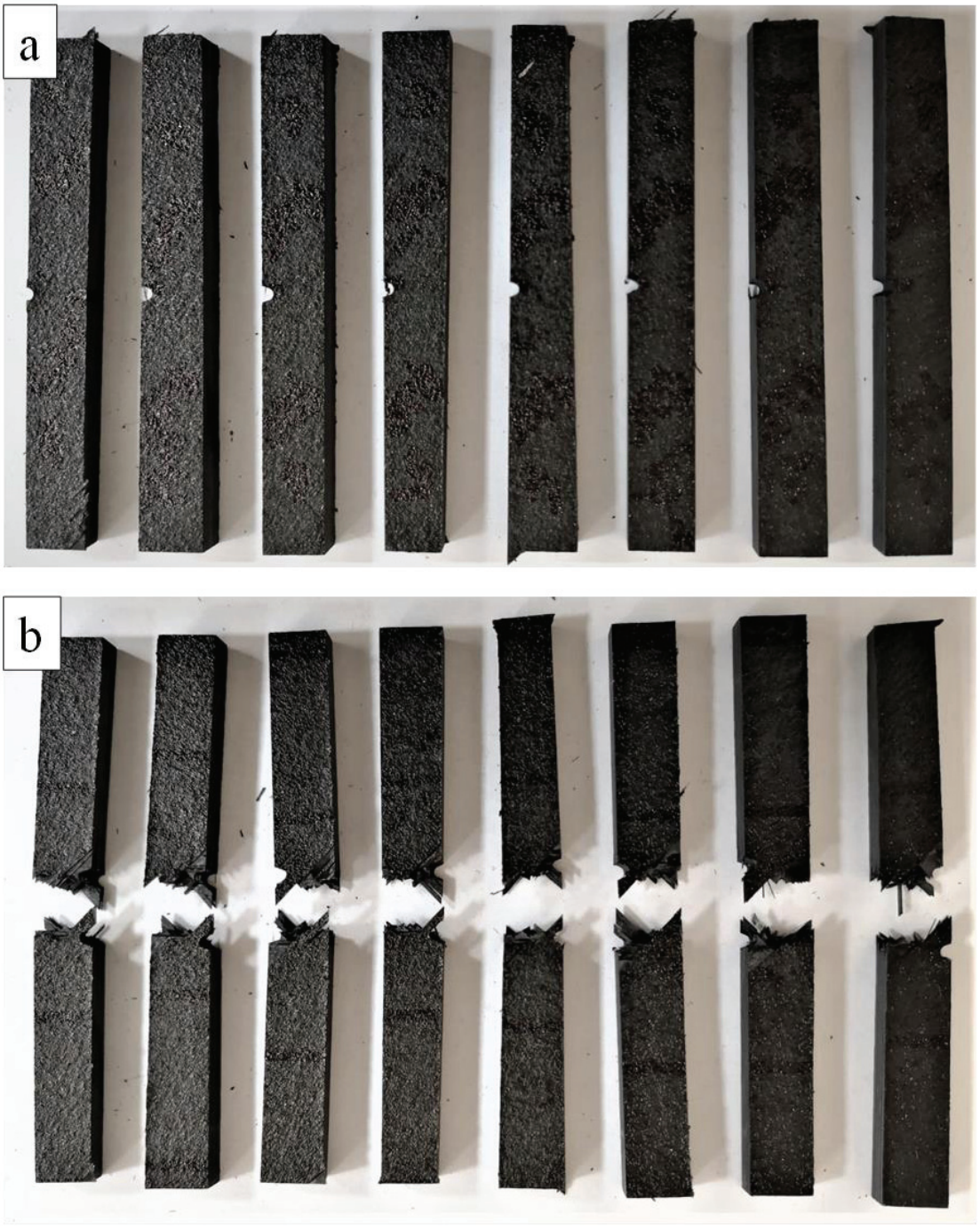

Figure 3. 12. Impact test reference specimen A (laser surface modification with 0.15 mm laser offset distance) produced with the secondary bonding method a) Before the test b) After the test

The pre-test and post-test images of the samples with laser surface modification at 0.20 mm laser offset distance are shown in Figure 3.13. Charpy impact test results were calculated based on the cross-sectional area of the test specimens.

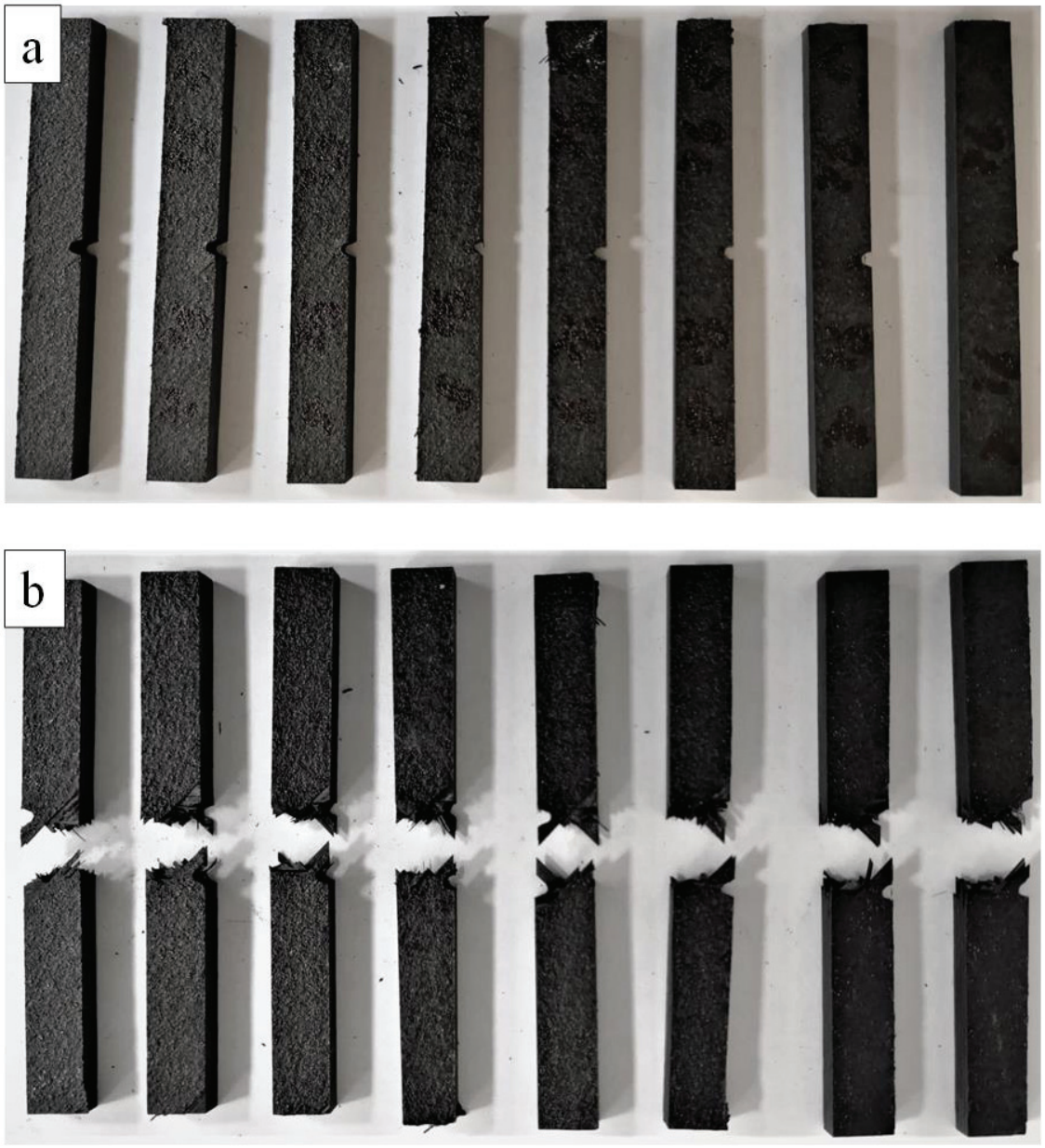

Figure 3. 13. Impact test reference specimen B (laser surface modification with 0.20 mm laser offset distance) produced with the secondary bonding method a) Before the test b) After the test

The pre- and post-test images of the samples with laser surface modification at 0.25 mm laser offset distance are shown in Figure 3.14. Charpy impact test results were calculated based on the cross-sectional area of the test specimens.

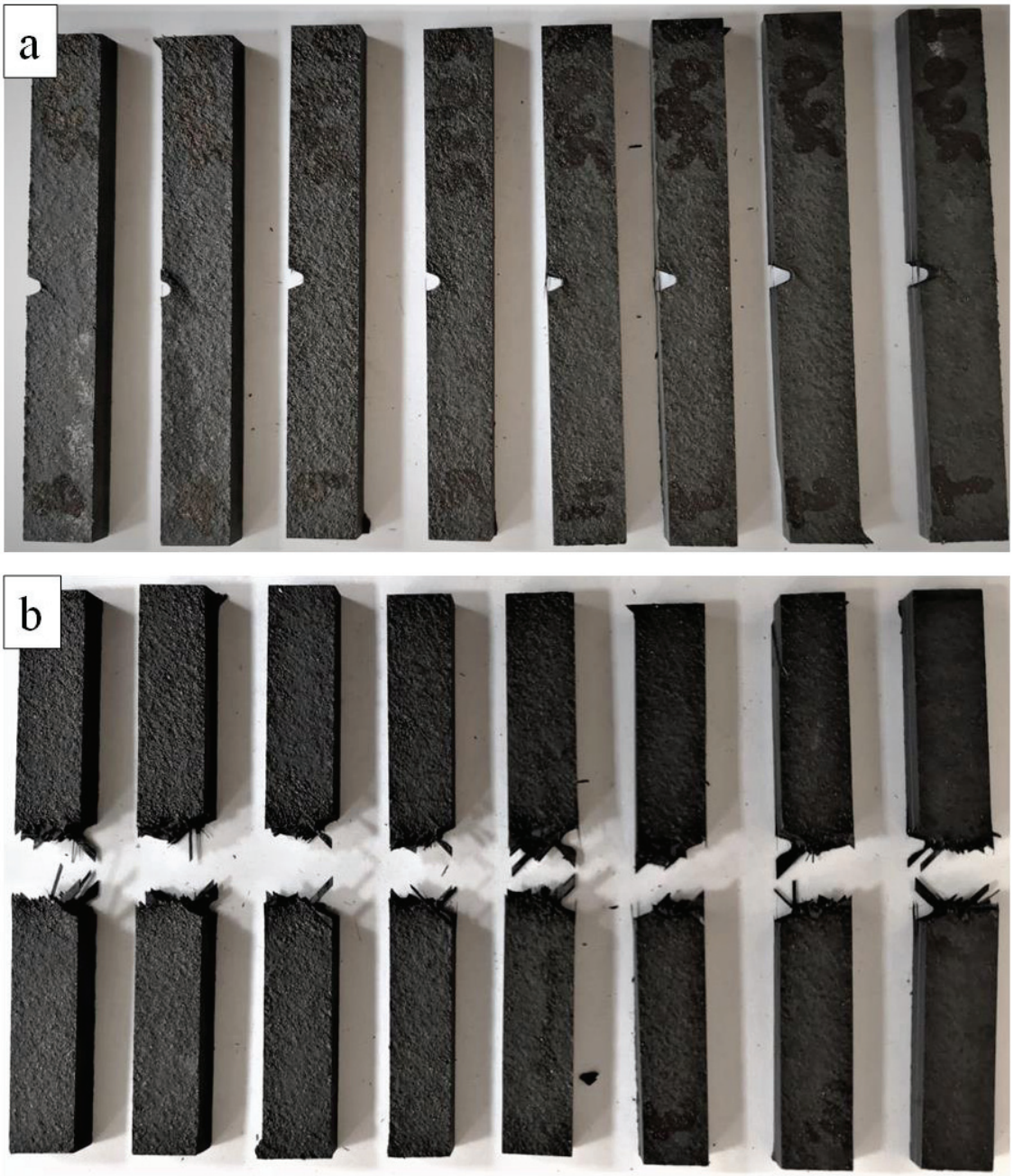

Figure 3. 14. Impact test reference specimen C (laser surface modification with 0.25 mm laser offset distance) produced with the secondary bonding method a) Before the test b) After the test

Table 3.2 shows the Charpy impact experiment results. The average Charpy impact energy of the reference composite samples was determined as 93.03 kJ/m2. The average Charpy impact energy of the laser modified composite samples with 0.15 mm laser offset distance was determined as 91.06 kJ/m2. The average Charpy impact energy of the laser modified composite samples with a laser offset distance of 0.20 mm was determined as 113.17 kJ/m2. The average Charpy impact energy of the laser modified composite samples with a laser offset distance of 0.25 mm was determined as 98.73 kJ/m2. By applying laser modification to the reference composites, the charpy-impact energy was increased by approximately 21.66%.

Table 3. 2. Charpy Impact Results

Sample	Charpy Impact Energy (kJ/m2)			
	Reference	A (0.15 mm Laser Offset Distance)	B (0.20 mm Laser Offset Distance)	C (0.25 mm Laser Offset Distance)
1	95.87	91.62	122.67	105.78
2	91.32	92.78	116.16	99.19
3	75.58	90.59	105.84	95.93
4	98.54	95.79	99.66	98.78
5	92.34	87.71	106.46	94.46
6	101.28	95.00	125.07	97.52
7	94.32	90.69	118.91	103.38
8	94.97	84.27	110.63	94.82
Avarage	93.03	91.06	113.17	98.73
Standard Deviation	7.74	3.76	8.96	4.04
Improvement(%)	-	-2.12	21.66	6.13

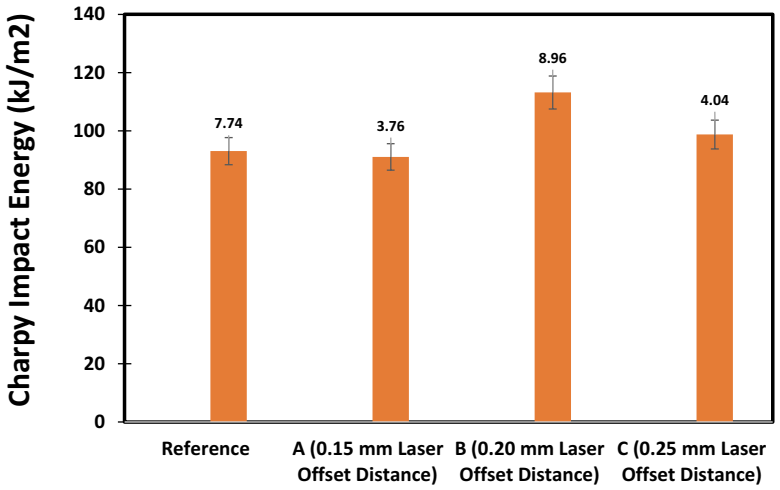

Figure 3. 15. Charpy impact energy of composite test specimens

Figure 3.16 shows post-test SEM images of laser surface modified composites with reference and 0.20 mm laser offset distance after charpy impact test. When the fracture surfaces were examined, it was observed that the samples with laser surface modification were more fragmented than the reference sample.

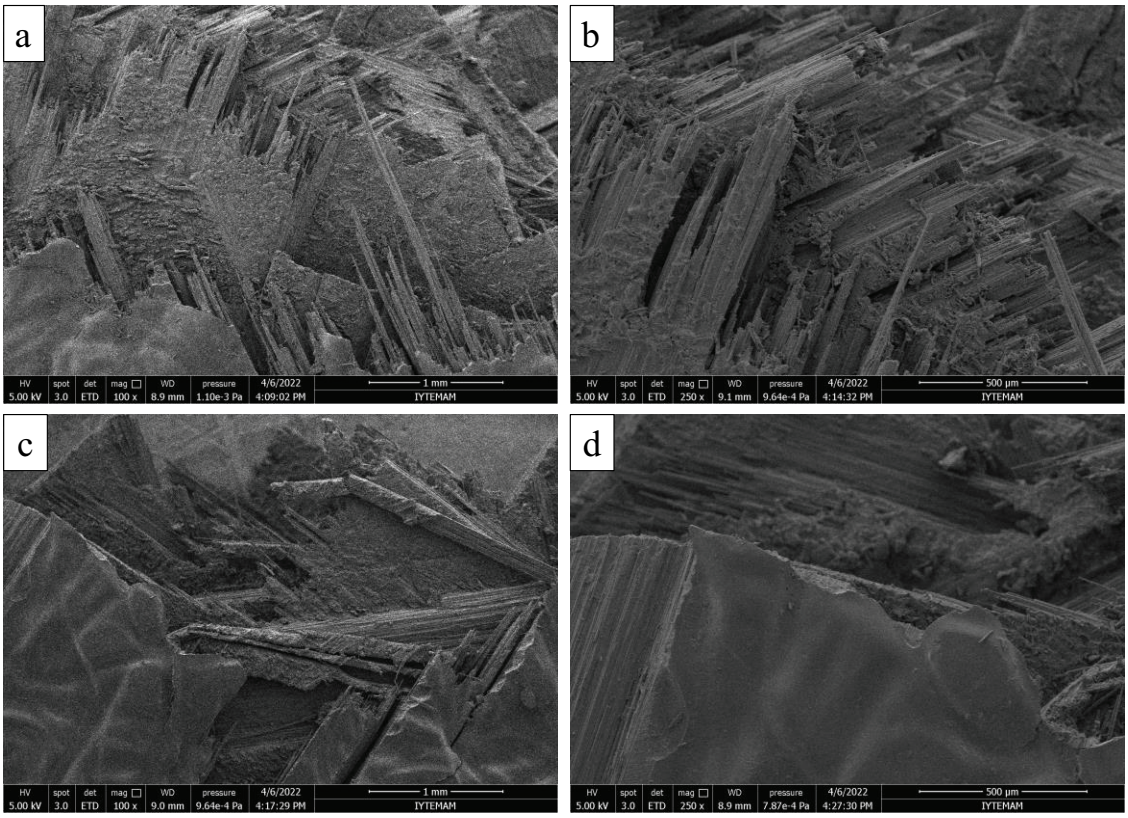

Figure 3. 16. SEM images of fracture surface charpy impact samples a, b) reference sample c,d) sample B at different magnification a, c)100x, b, d)250x

3.3. Mode-I Fracture Toughness Test

Figure 3.17 shows the G_{IC} and delamination length curve of laser surface modified composite samples with reference and laser offset distance of 0.20 mm. The crack initiation and propagation values for the reference samples were calculated as 0.04 and 0.34 kJ/m2, respectively. The maximum G_{IC} value of the reference composites was determined as 0.95 kJ/m2. The crack initiation and propagation Mode-I fracture toughness values were calculated as 0.03 and 0.44 kJ/m2, respectively, for composites undergone laser surface modification with a laser offset distance of 0.20 mm. The

maximum G_{IC} value of laser surface modified composites was determined as 0.82 kJ/m2. When the laser surface modified samples were compared with the reference samples, it was determined that the Mode-I fracture toughness value increased by approximately 30.39%.

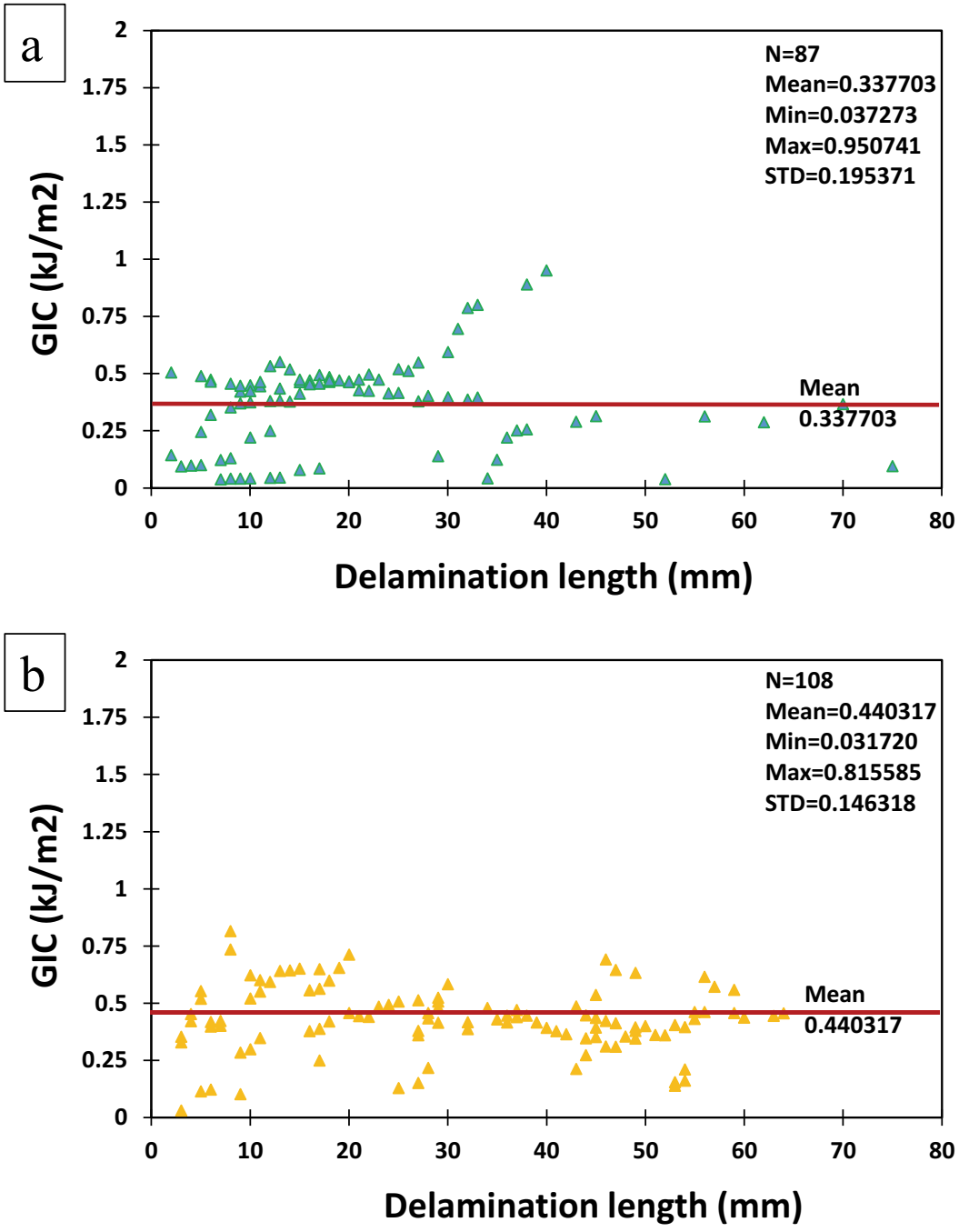

Figure 3. 17. G_{IC} and delamination length curve of a) reference sample and b) sample B (laser surface modified with 0.20 mm laser offset distance).

Table 3. 3. Mode-I fracture toughness test results

Sample Name	Mode-I fracture toughness	Mode-I fracture toughness	Max. Mode-I fracture toughness
	G_{ICini} (kJ/m^2)	G_{ICprop} (kJ/m^2)	$G_{ICmax.}$ (kJ/m^2)
Reference Avg.	0.04	0.34	0.95
B (Laser Modified Avg.)	0.03	0.44	0.82
Improvement (%)	-	30.39	-

Figure 3.18 shows the fracture surfaces of the composite specimens with laser surface modification with reference and 0.2 mm laser offset distance after DCB test. Compared to the reference samples, the laser surface modified composite samples showed a different type of fracture behavior. When looking at the reference samples, the separation took place in the adhesion region, while in the composite samples with laser surface modification, the separation started in the adhesive first and passed to the UD composite side. This supports that by laser modification, the adhesive further penetrates the fibers, increasing the adhesion performance.

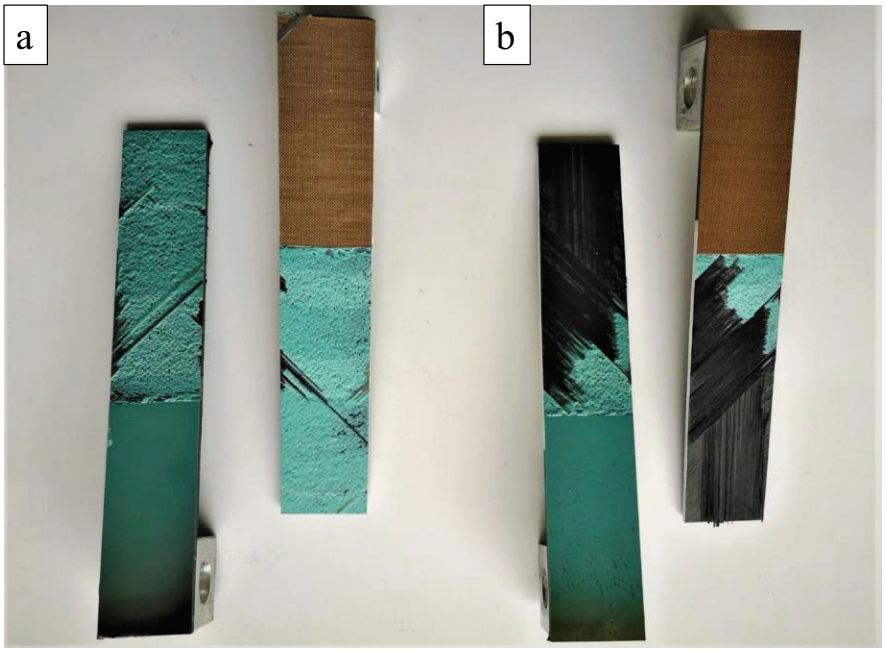

Figure 3. 18. Photograph of the DCB surfaces of fractured a) reference sample and b) sample B (laser treated with 0.20 mm laser offset distance).

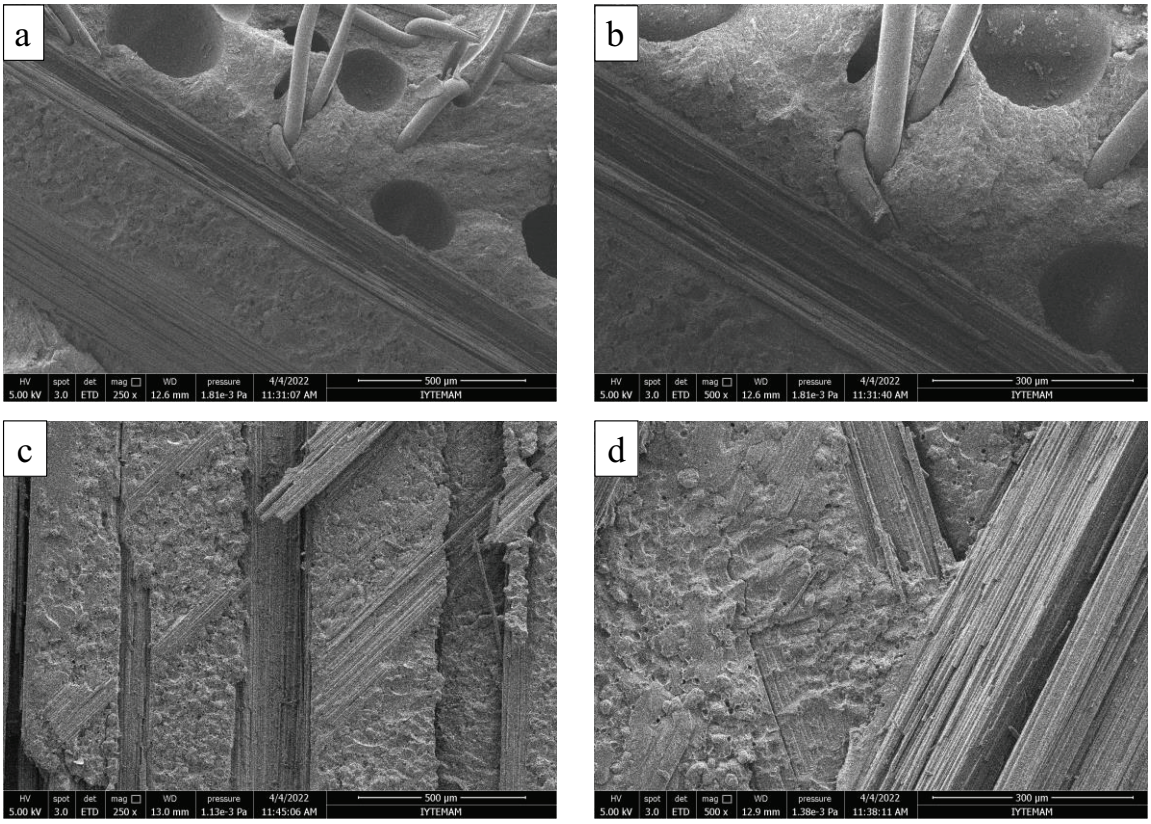

Figure 3. 19. SEM images of fracture surface Mode-I samples a, b) reference sample and c,d) sample B (laser surface treatment) at different magnification a, c)250x, b, d)500x

3.4. Single Lap Shear Test After Aging

Shear strength properties of composite specimens after aging whose joint area was modified by laser ablation were investigated. Laser ablation was performed on the adhesion surfaces of the plates with 20 mm laser offset distance. Samples were prepared to evaluate the adhesion strength of UD prepreg plates after 1.5 months aging adhered with FM300K film adhesive. Single lap shear tests were performed with ASTM D5868.

The images of the single-lap shear test after aging of the reference samples are shown in Figure 3.20. Single lap shear results were calculated based on the cross-sectional area of the test specimens.

Figure 3. 20. Single lap shear reference test specimen after environmental aging

The images of the single-lap shear test after aging of the samples with laser surface modification at 0.20 mm laser offset distance are shown in Figure 3.21. Single lap shear test results were calculated based on the cross-sectional area of the test specimens.

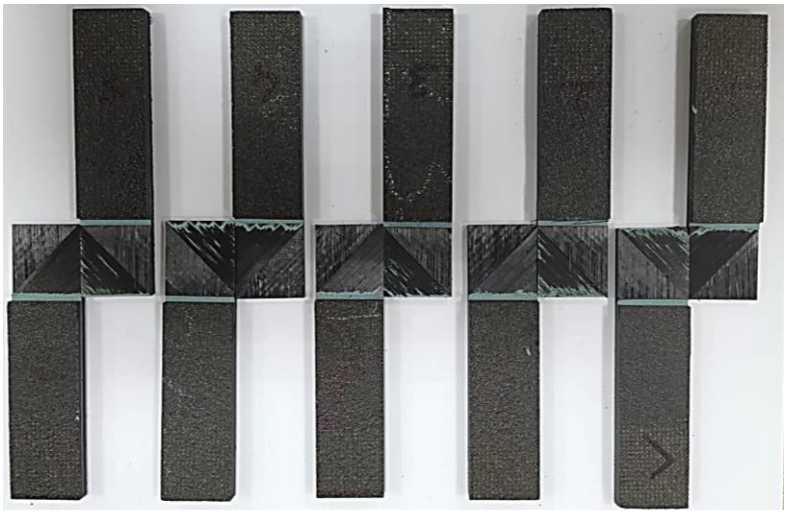

Figure 3. 21. Single lap shear test specimen B (laser surface modification with 0.20 mm laser offset distance) after environmental aging

Lap shear test results after aging of composite specimens with laser surface modification are shown in Table 3.4. The average shear strength of the reference samples is 17.09 MPa. The average shear strength of the reference samples after aging decreased by 9.71 percent compared to the reference sample and was 15.43 MPa. The average shear strength of the samples with laser surface modification is 19.46 MPa. The shear strength of laser ablated sample after aging with the 0.20 mm laser offset distance showed an decrease of 5.29% compared to the laser ablated sample and was 18.43 MPa. The shear strength of the laser ablated sample with 0.20 laser offset distance showed an improvement of 7.59% compared to the reference sample and was 18.39 MPa. After aging, the lap shear strength of the samples with laser surface modification with a laser offset distance of 0.20 mm increased compared to the reference sample after aging. When the test results in Table 4.4 are examined, in both conditions, an increase in the shear strength of the laser surface modified samples is observed. The laser surface modification process has proven to show a dramatic increase in shear strength. The resulting structure is a good method to reduce joint site fragility.

Table 3. 4. Lap Shear Test Results

Sample	Shear Strength After Aging (Mpa)		Shear Strength (Mpa)	
	Reference	B (0.20 mm Laser Offset Distance)	Reference	B (0.20 mm Laser Offset Distance)
1	14.22	18.81	16.71	19.07
2	13.54	14.92	16.37	19.16
3	17.28	20.35	17.00	19.77
4	17.48	19.05	17.73	19.44
5	14.64	19.05	17.64	19.86
Avarage	15.43	18.43	17.09	19.46
Standard Deviation	1.82	1.83	0.59	0.35
Reduction due to aging(%)	9.71	5.29	-	-

Shear load-extension diagrams of reference samples after environmental aging are shown in Figure 3.22. Single lap shear test results were calculated based on the force-displacement curve and the cross-sectional area of the test specimens.

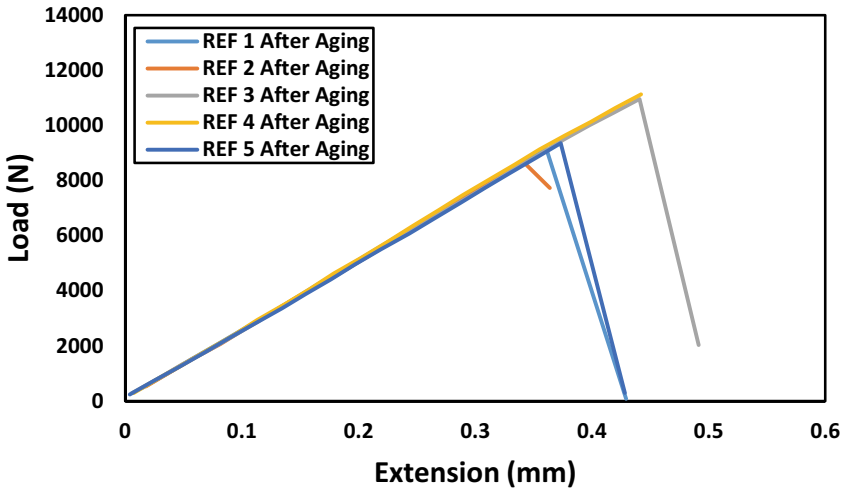

Figure 3. 22. Load vs. extension curves of reference specimens after environmental aging according to single lap shear test.

Shear load-extension diagrams of laser treated with 0.20 laser offset distance samples after environmental aging are shown in Figure 3.23. Single lap shear test results were calculated based on the force-displacement curve and the cross-sectional area of the test specimens.

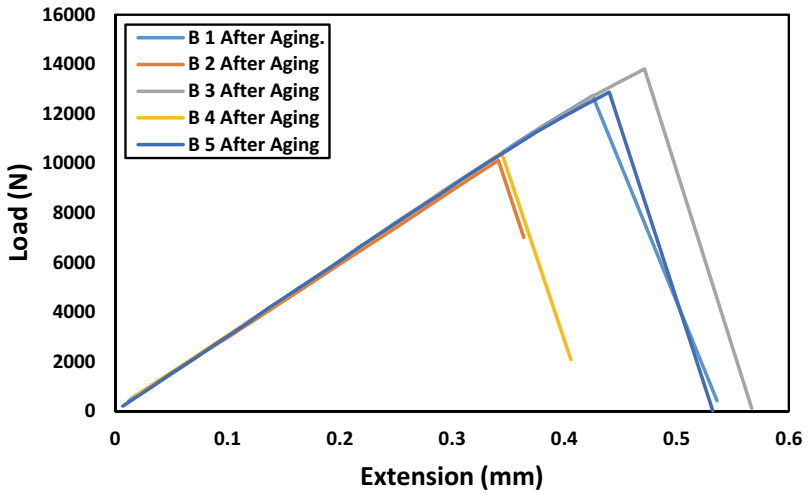

Figure 3. 23. Load vs. extension curves of laser surface treated with 0.20 mm laser offset distance specimens after environmental aging according to single lap shear test.

When the fracture surfaces of the joint area of the specimens with lap shear test after aging were examined, it was observed that the adhesive of the specimens with laser surface modification was more penetrating into the fiber compared to the reference specimens, just as in the first lap shear test.

Figure 3.24 and Figure 3.25 show the joint area and SEM images of the reference and laser surface modified composites after environmental aging after the lap shear test. When the fracture surfaces of the joint area were examined, it was observed that the laser-modified samples adhered better. When the junction region of the reference sample was examined after environmental aging, it was observed that the fracture mode was adhesive rupture as in the case of no aging. When the joint region of the composite sample, which underwent laser surface modification with a laser offset distance of 0.20 mm, was examined after environmental aging, it was observed that the fracture mode was fiber-tier error, just as in the case of no aging. In these samples, it was determined that the adhesive increased the bond strength by penetrating more fibers. When the test results were examined, it was proved that the laser surface modification treatment showed a nice increase in bond strength even after environmental aging. Laser surface modification is a good method to reduce joint area fragility.

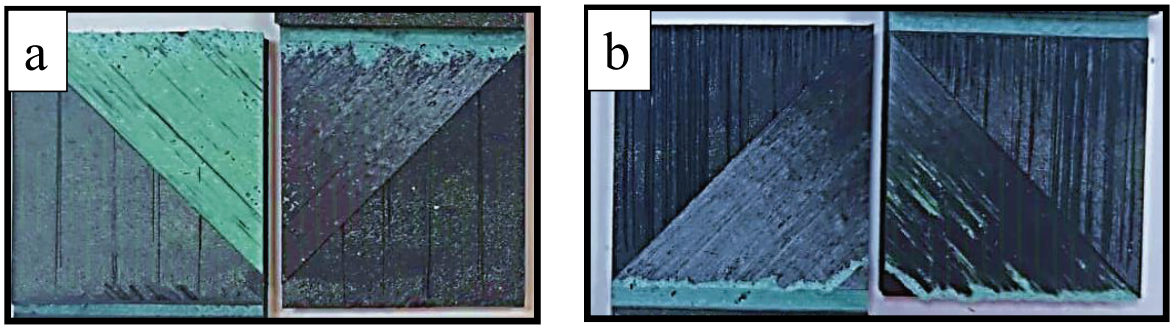

Figure 3. 24. The fracture surface after single lap shear test of a) reference sample, b) sample B (laser treated with 0.20 mm offset distance) after environmental aging

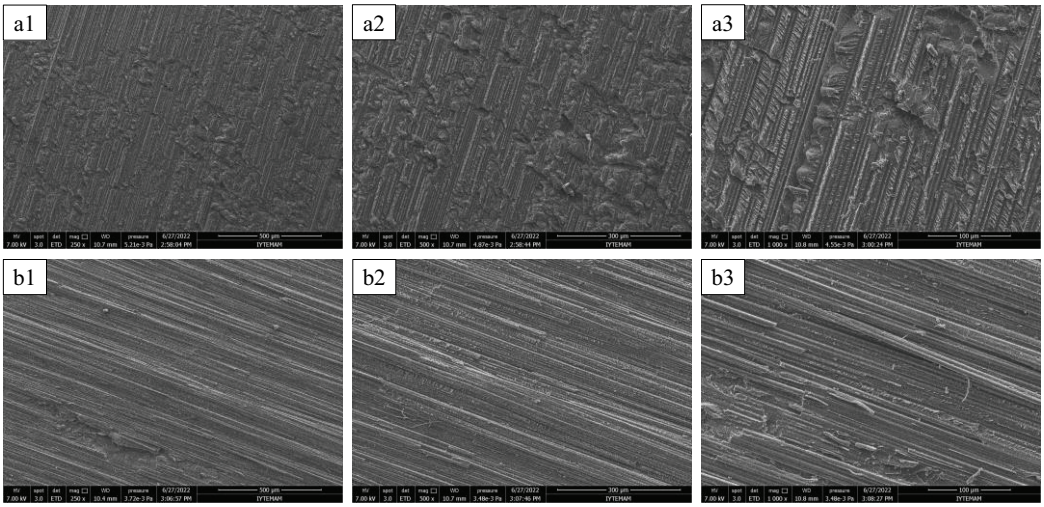

Figure 3. 25. Shows the junction region SEM images after single lap shear test at different magnification 1) 250x, 2) 500x, and 3) 1000x of the a) reference sample, b) B sample (laser treated with 0.20 mm offset distance) after environmental aging

3.5. Charpy Impact Test After Aging

The charpy impact energy properties of after enviromental aging composite specimens whose joint area was modified by laser ablation were investigated. Charpy impact tests were carried out with the ISO-179 standard. Samples were prepared to evaluate the adhesion strength of UD prepreg plates adhered with FM300K film adhesive. Laser ablation was performed on the adhesion surfaces of the plates with 0.20 laser offset distance. It was then kept in an environmental aging cabinet at 85% humidity and 70 °C for 1.5 months.

The images of the reference charpy impact post-test sample after aging the are shown in Figure 3.26. Results are calculated based on the cross-sectional area of the test specimens.

The post-test images of the laser surface modified samples after environmental aging with 0.20 laser offset distance are shown in Figure 3.27. Charpy impact energy test results were calculated based on the cross-sectional area of the test specimens.

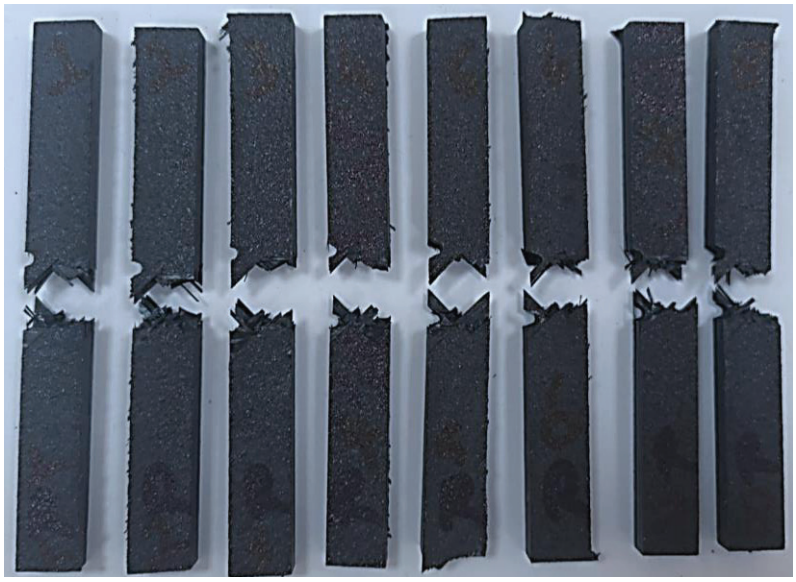

Figure 3. 26. Post-test image of aged Charpy impact reference test specimen produced by secondary bonding method

The post-test images of the laser surface modified samples after environmental aging with 0.20 laser offset distance are shown in Figure 3.27. Charpy impact energy test results were calculated based on the cross-sectional area of the test specimens.

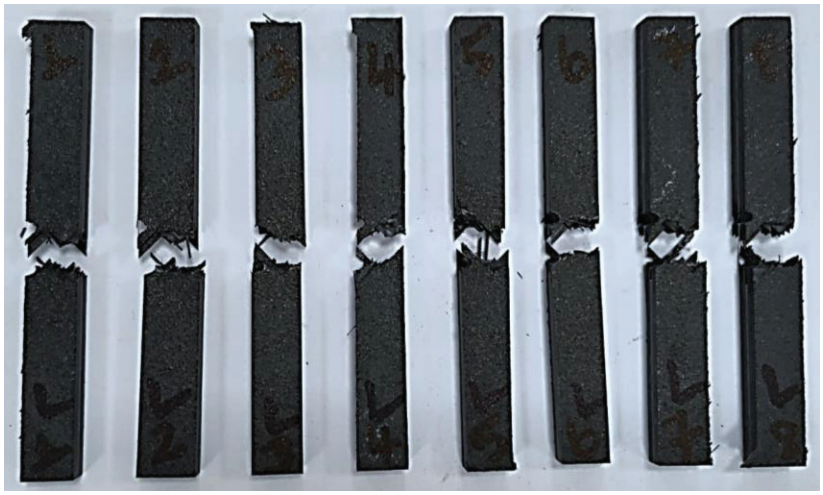

Figure 3. 27. Post-test image of aged Charpy impact test specimen B produced by secondary bonding method (laser surface modification with 0.20 mm laser offset distance)

Table 3.5 shows the Charpy experiment results. The average Charpy impact energy of the reference composite samples was determined as 93.03 kJ/m2. The average Charpy impact energy of the reference composite samples after aging was determined as 91.64 kJ/m2. The average Charpy impact energy of the laser modified composite samples with a laser step pitch of 0.20 was determined as 113.17 kJ/m2. The average Charpy impact energy of the composite samples after laser modified aging with a laser step pitch of 0.20 was determined as 98.02 kJ/m2. By applying environmental aging to the reference composites, the impact energy was reduced by approximately 1.51%. By applying aging to the samples with 0.20 mm laser offset distance, the impact energy was reduced by about 15.46%. When Table 3.5 and Figure 3.28 were examined, it was seen that aging did not make a significant difference on charpy impact energy.

Table 3. 5. Charpy Impact Test Results

Sample	Charpy Impact Energy (kJ/m2)			
	After Aging		-	
	Reference	B (0.20 mm Laser Offset Distance)	Reference	B (0.20 mm Laser Offset Distance)
1	91.70	98.97	95.87	122.67
2	92.55	102.11	91.32	116.16
3	92.72	90.12	75.58	105.84
4	92.17	87.52	98.54	99.66
5	90.83	102.19	92.34	106.46
6	85.46	103.69	101.28	125.07
7	93.44	104.07	94.32	118.91
8	94.28	95.54	94.97	110.63
Avarage	91.64	98.02	93.03	113.17
Standard Deviation	2.71	6.35	7.74	8.96
Reduction(%)	1.51	15.46	-	-

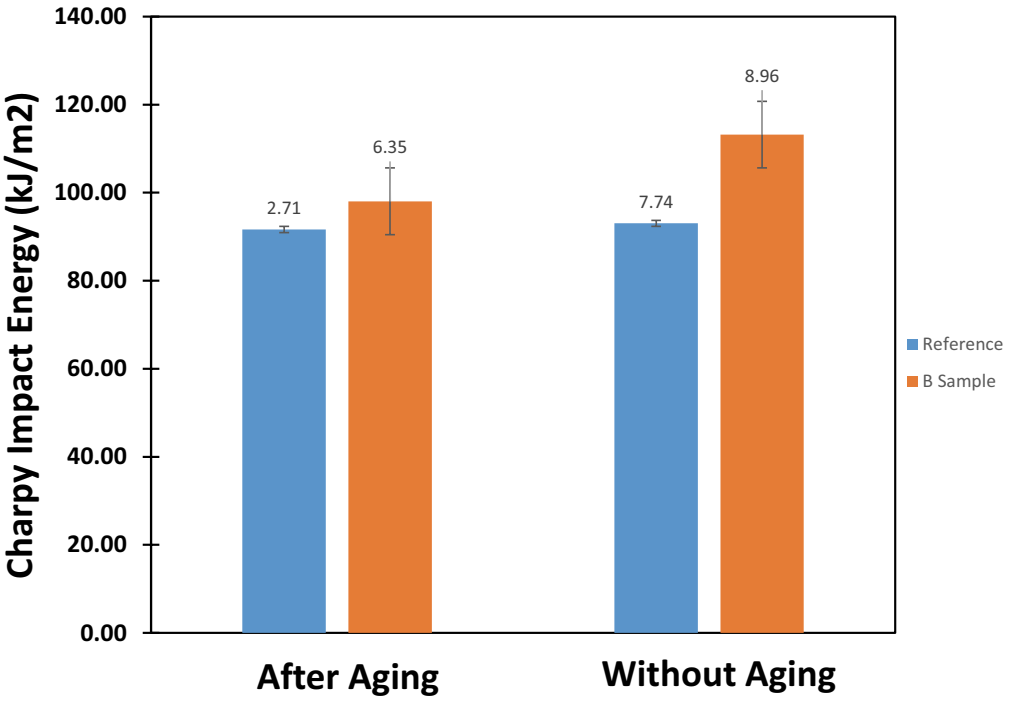

Figure 3. 28. Charpy impact energy of composite test specimens after aging

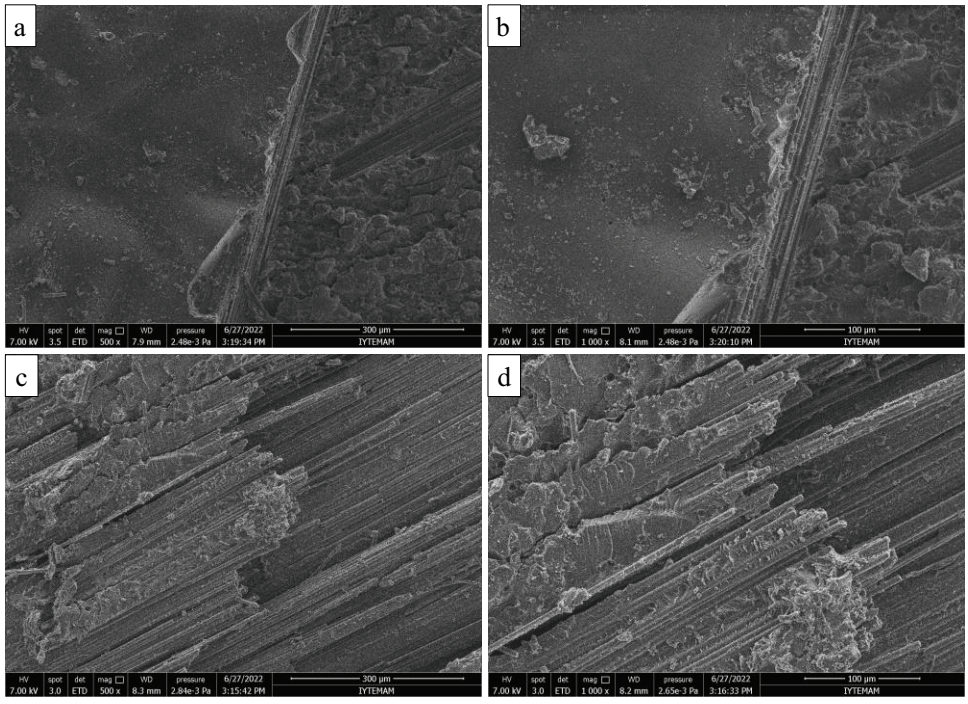

Figure 3. 29. SEM images of fracture surface charpy samples after aging a, b) reference sample and c,d) sample B (laser surface treatment) at different magnification a, c)500x, b, d)1000x

3.6. Mode-I Fracture Toughness Test After Aging

Figure 3.30 shows the G_{IC} and delamination length curve of laser surface modified composite samples after environmental aging with laser offset distance of 0.20 mm and reference. The crack initiation and propagation values for the reference samples after environmental aging were calculated as 0.42 and 1.48 kJ/m2, respectively. The maximum G_{IC} value of the reference composites after environmental aging was determined as 2.89 kJ/m2. The crack initiation and propagation Mode-I fracture toughness values were calculated as 0.46 and 1.89 kJ/m2, respectively, for composites after environmental aging with laser surface modification with a laser offset distance of 0.20 mm. The maximum G_{IC} value of laser surface modified composites after environmental aging was determined as 3.25 kJ/m2.

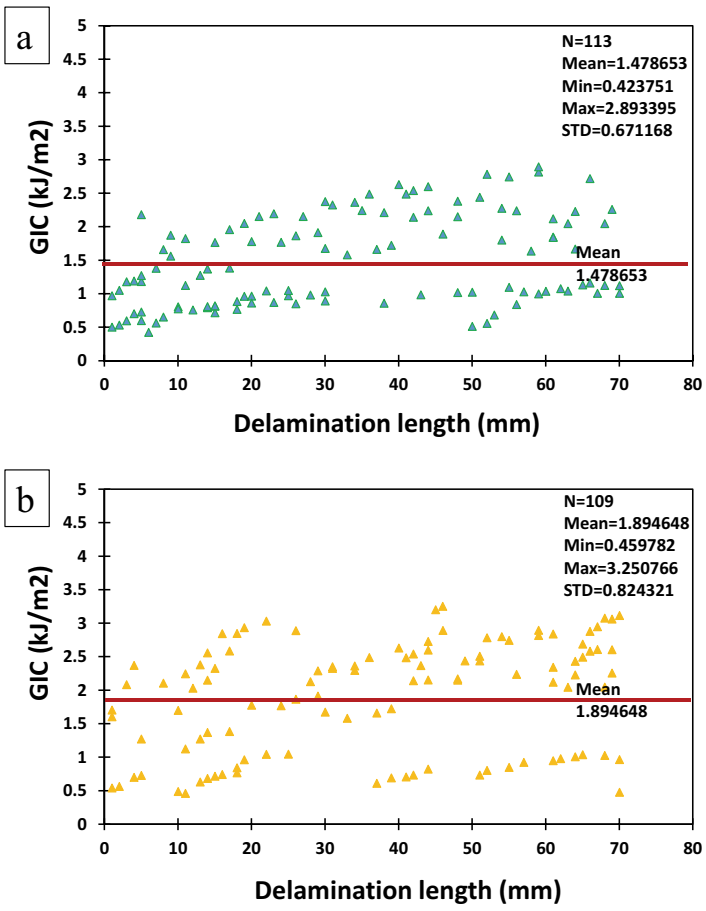

Figure 3. 30. G_{IC} and delamination length curve of a) reference sample and b) B sample (laser surface modified with 0.20mm laser offset distance) after aging.

When the laser surface modified samples after environmental aging were compared with the reference samples after aging, it was determined that the Mode-I fracture toughness value increased by approximately 28.57% (Table 4.6).

Table 3. 6. Mode-I fracture toughness test results after aging

Sample Name	After Aging		
	Mod-I fracture toughness	**Mod-I fracture toughness**	**Max. Mod-I fracture toughness**
	G_{ICini} (kJ/m^2)	**G_{ICprop} (kJ/m^2)**	**$G_{ICmax.}$ (kJ/m^2)**
Reference Avg.	0.42	1.48	2.89
Laser Modified Avg.	0.46	1.89	3.25
Improvement(%)	-	28.57	-

When Table 3.7 is examined, an increase of 335.29% was observed in the fracture toughness of sample, which was exposed to environmental aging conditions, compared to the reference sample. There was a 329.25% improvement in fracture toughness in the samples with laser surface modification and environmental aging compared to the samples with laser surface modification. Çevresel yaşlandırma koşullarından referans ve lazer yüzey modifiyeli numune benzer oranlarda etkilenmişlerdir. Reference and laser surface modified samples were affected by environmental aging conditions at similar rates.

Table 3. 7. Mode-I fracture toughness test results after aging

Sample Name	**After Aging**		**Improvement(%)**
	Mod-I fracture toughness	**Mod-I fracture toughness**	
	G_{ICprop} (kJ/m^2)	**G_{ICprop} (kJ/m^2)**	
Reference Avg.	1.48	0.34	**335.29**
B (Laser Modified Avg.)	1.89	0.44	**329.55**
Improvement(%)	**28.57**	**30.39**	

Figure 3.31 shows the fracture surfaces of the composite specimens after environmental aging with laser surface modification with reference and 0.2 laser offset distance after DCB test. Compared to the reference samples after environmental aging, the laser surface modified composite samples after environmental aging showed a different type of fracture behavior. When looking at the reference samples, the separation took place in the adhesion region, while in the composite samples with laser surface modification, the separation started in the adhesive first and passed to the UD composite side. This supports that by laser modification, the adhesive further penetrates the fibers, increasing the adhesion performance.

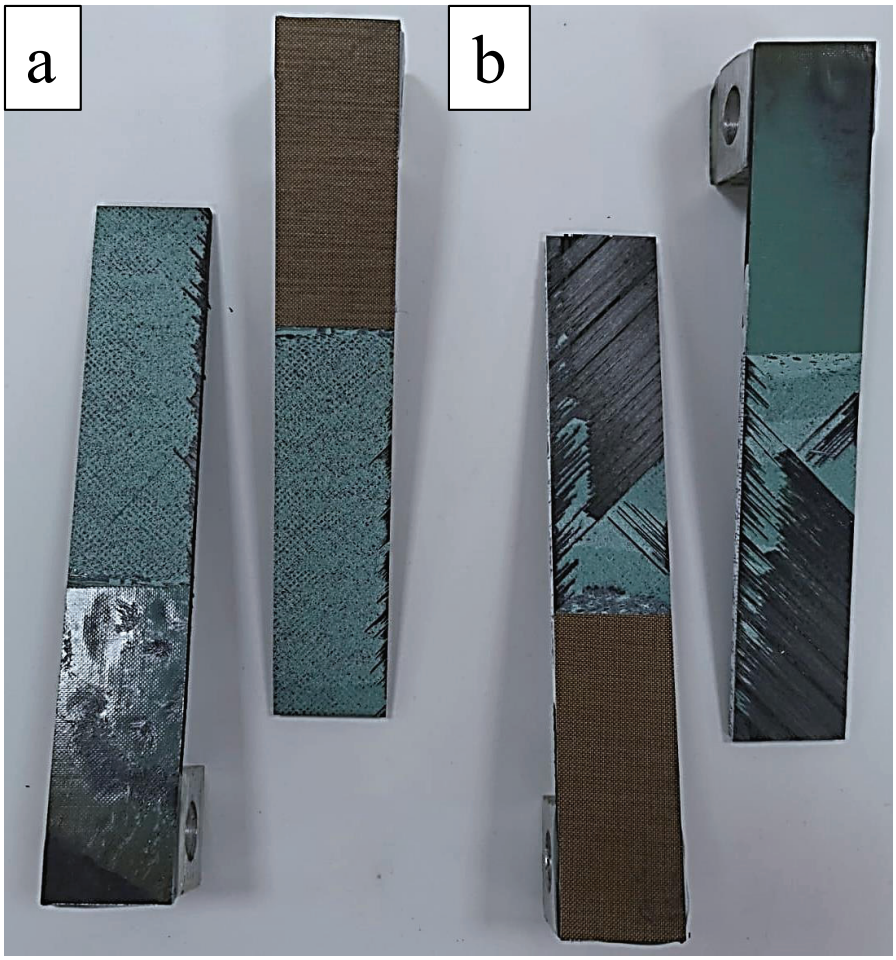

Figure 3. 31. Photograph of fractured surfaces of DCB specimens after aging a) reference sample and b) sample B (laser treatment with 0.20 mm laser offset distance).

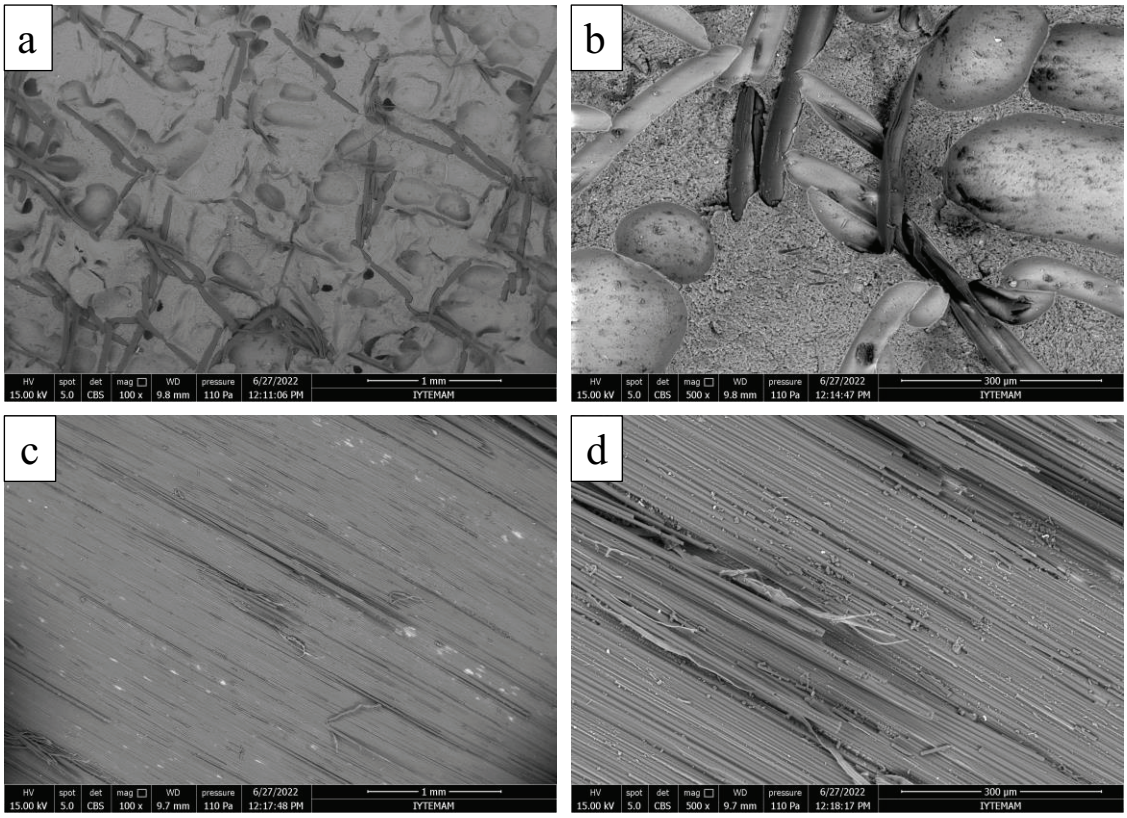

Figure 3. 32. SEM images of fracture surface Mode-I samples after aging a, b) reference sample and c,d) sample B (laser surface treatment) at different magnification a, c)100x, b, d)500x

CHAPTER 4

CONCLUSIONS

In this thesis, it is aimed to reduce the production-induced pollution on the surfaces of composite materials in order to increase the adhesive bonding performance of composite/composite connections used in aviation, and thus to increase the adhesion strength. For this purpose, the first step is the aim was to determine the parameters that can remove the epoxy from the surface of the selected plate without damaging the fibers. In this thesis, nanosecond pulsed fiber laser was used. After many studies carried out for the purpose, the lowest energy at which the epoxy can be moved away from the surface was aimed. After establishing the energy equation of a single laser pulse with the inputs of the laser device, the lowest power that can remove the epoxy was chosen. The highest speed and lowest frequency at which the device works effectively are selected. In order to examine the effect of the total energy applied to the surface on the adhesion performance, laser surface treatment with 3 different offset distances was applied to the CFRP plates. In order to analyze the effect of the total energy applied to the surface on the adhesion performance, optical microscope and SEM images were taken and contact angle tests were also carried out. After observing the ability of laser pulses to remove epoxy in an optical microscope, SEM images were examined. In the SEM images, it was observed that the epoxy was completely removed from the surface with the laser pulse without damaging the fibers.

Today, two different adhesives, thin film and liquid, are used for bonding composite materials. Each adhesive has its own advantages and disadvantages. Since thin-film adhesives generally provide higher strengths in adhesion, it was decided to use a film adhesive. Two CFRP composite plates with laser surface modification using film adhesive were joined secondary bonding by hot press method.

Lap shear, charpy impact and DCB mechanical tests were carried out to see the mechanical effects on adhesion performance. According to the lap shear tests, the laser offset distance in which the shear strength increased the most was determined as 0.20

mm. The shear strength of the samples with laser surface modification with 0.20 mm laser offset distance is 13.87% higher than the strength of the reference samples without laser surface modification. When the refraction modes of different laser offset distances were examined, it was observed that the samples with laser surface treatment with a laser offset distance of 0.15 mm were refracted from the fibers. In line with this observation, it was observed that the total laser energy at 0.15 mm laser offset distance damaged the fibers, so the shear strength decreased compared to the sample without laser surface modification. When the refraction modes of the reference samples without laser surface modification were examined, it was observed that there was adhesive failure. When the refraction modes of the samples with laser surface modification with 0.25 mm laser offset distance were examined, it was observed that there was light-tear failure. In the samples with laser surface treatment with 0.25 mm laser offset distance, the adhesive penetrated more than the reference samples, so the shear strength increased by 7.59%. Fiber-tear failure was observed when the refraction modes of the samples, on which laser surface modification was made with a laser offset distance of 0.20 mm, were examined. In the samples with laser surface treatment with 0.20 mm laser offset distance, the adhesive penetrated the fibers more than the reference samples, so the shear strength increased by 13.87%. The charpy impact energy of the samples with laser surface modification with a laser offset distance of 0.20 mm increased by 21.66% compared to the impact strength of the samples without laser surface treatment. The fracture toughness of the samples with laser surface treatment with 0.20 mm laser offset distance increased by %30.39 compared to the fracture toughness of the samples without laser surface treatment. The reason for this increase is that while separation takes place from the adhesive in the reference samples, in the laser modified samples, the separation first starts from the adhesive and then continues from the material. This shows that the adhesion of the fibers with the adhesive increases.

The second aim is to investigate the effect of the adhesion performance of the laser surface modified plates under the flight conditions to which the aircraft is exposed. In line with this aim, the plates were kept in the environmental chamber for 1.5 months at 85% humidity and 70°C. Lap shear, charpy impact and DCB mechanical tests were performed to examine the effects of environmental aging conditions on the adhesion performance of laser surface modified samples. The shear strength of the reference samples after

environmental aging is 9.71% lower than the shear strength of the reference samples. After environmental aging, the shear strength of the samples with laser surface modification is 5.29% lower than the shear strength of the samples with laser surface modification. Laser surface modification shows less reduction under environmental effects than the reference sample. The charpy impact energy of the reference samples after environmental aging is 1.51% lower than the charpy impact energy of the reference samples. The charpy pulse energy of the samples with laser surface modification after environmental aging is 0.72% lower than the charpy pulse energy of the samples with laser surface modification. It was observed that environmental effects did not make a significant difference for charpy impact energy. The fracture toughness of the reference samples after environmental aging is 335.29% higher than the fracture toughness of the reference samples. The fracture toughness of the laser surface modification samples after environmental aging is 329.55% higher than the fracture toughness of the laser surface modification samples. Laser surface modification shows more improvement under environmental effects than the reference sample. Although laser surface modified composite plates and reference composite plates are similarly affected by environmental aging conditions in terms of mechanical performance, laser surface modified and aged composite plates still have higher performance than reference aged plates. This makes it meaningful to choose the laser surface modification process.

4.1. Future Works

- Tensile, compression and 3-point bending tests will be done.
- Tensile, compression and 3-point tests will be performed on the aging samples in order to analyze them under environmental aging.
- The fatigue behavior of reference and laser samples will be examined.
- Test coupons will be produced by autoclave method and then mechanical tests will be done.
- The epoxy on the entire surface will be removed by laser, then the grove will be created using the laser method and new laser parameters will be tested.

- To compare the applicability of the data in our study, sample production and analysis combined with mechanical methods (Al-based riveting - fasteners, etc.) will be performed.

REFERENCES

(1) F.C. Campbell. Chapter 1: Introduction to Composite Materials. In *Structural Composite Materials*; 2010; pp 1–29.

(2) Biswal, T.; BadJena, S. K.; Pradhan, D. Synthesis of Polymer Composite Materials and Their Biomedical Applications. *Mater. Today Proc.* **2020**, *30*, 305–315. https://doi.org/10.1016/j.matpr.2020.01.567.

(3) Nagavally, R. R. Composite Materials - History, Types, Fabrication Techniques, Advantages, and Applications. *Int. J. Mech. Prod. Eng.* **2016**, 25–30.

(4) Sun, C.; Min, J.; Lin, J.; Wan, H.; Yang, S.; Wang, S. The Effect of Laser Ablation Treatment on the Chemistry, Morphology and Bonding Strength of CFRP Joints. *Int. J. Adhes. Adhes.* **2018**, *84* (April), 325–334. https://doi.org/10.1016/j.ijadhadh.2018.04.014.

(5) Li, X.; Ehrhardt, M.; Lorenz, P.; Han, B.; Lai, S.; Zimmer, K.; Xu, L.; Nan, P.; Ni, X. Influence of Surface Treatment with Infrared Nanosecond Laser on Adhesion Performance of Adhesion-Bonded Carbon Fiber/Epoxy Composite. *J. Adhes. Sci. Technol.* **2020**, *34* (13), 1399–1425. https://doi.org/10.1080/01694243.2019.1710990.

(6) Fischer, F.; Kreling, S.; Jäschke, P.; Frauenhofer, M.; Kracht, D.; Dilger, K. Laser Surface Pre-Treatment of CFRP for Adhesive Bonding in Consideration of the Absorption Behaviour. *J. Adhes.* **2012**, *88* (4–6), 350–363. https://doi.org/10.1080/00218464.2012.660042.

(7) Xie, Y.; Yang, B.; Lu, L.; Wan, Z.; Liu, X. Shear Strength of Bonded Joints of Carbon Fiber Reinforced Plastic (CFRP) Laminates Enhanced by a Two-Step Laser Surface Treatment. *Compos. Struct.* **2020**, *232* (October 2019), 111559. https://doi.org/10.1016/j.compstruct.2019.111559.

(8) Li, S.; Sun, T.; Liu, C.; Yang, W.; Tang, Q. A Study of Laser Surface Treatment in Bonded Repair of Composite Aircraft Structures. *R. Soc. Open Sci.* **2018**, *5* (3). https://doi.org/10.1098/rsos.171272.

(9) Schweizer, M.; Meinhard, D.; Ruck, S.; Riegel, H.; Knoblauch, V. Adhesive Bonding of CFRP: A Comparison of Different Surface Pre-Treatment Strategies and Their Effect on the Bonding Shear Strength. *J. Adhes. Sci. Technol.* **2017**, *31* (23), 2581–2591. https://doi.org/10.1080/01694243.2017.1310695.

(10) Oliveira, V.; Sharma, S. P.; de Moura, M. F. S. F.; Moreira, R. D. F.; Vilar, R. Surface Treatment of CFRP Composites Using Femtosecond Laser Radiation. *Opt. Lasers Eng.* **2017**, *94* (February), 37–43. https://doi.org/10.1016/j.optlaseng.2017.02.011.

(11) Liang, L.; Lu, L.; Xing, D.; Wan, Z.; Tang, Y. Preparation of Superhydrophobic and Anti-Resin-Adhesive Surfaces with Micro/Nanoscale Structures on High-Speed Steel via Laser Processing. *Surf. Coatings Technol.* **2019**, *357* (October 2018), 57–68. https://doi.org/10.1016/j.surfcoat.2018.10.001.

(12) Shang, X.; Marques, E. A. S.; Machado, J. J. M.; Carbas, R. J. C.; Jiang, D.; da Silva, L. F. M. Review on Techniques to Improve the Strength of Adhesive Joints with Composite Adherends. *Compos. Part B Eng.* **2019**, *177* (November 2018), 107363. https://doi.org/10.1016/j.compositesb.2019.107363.

(13) Kusano, Y. Atmospheric Pressure Plasma Processing for Polymer Adhesion: A Review. *J. Adhes.* **2014**, *90* (9), 755–777. https://doi.org/10.1080/00218464.2013.804407.

(14) Molitor, P.; Barron, V.; Young, T. Surface Treatment of Titanium for Adhesive Bonding to Polymer Composites: A Review. *Int. J. Adhes. Adhes.* **2001**, *21* (2), 129–136. https://doi.org/10.1016/S0143-7496(00)00044-0.

(15) Robert D. Adams. Surface Treatments of Selected Materials. Handbook of Adhesion Technology. In *Handbook of Adhesion Technology*; Lucas F. M. da Silva, Andreas Öchsner, Ed.; 2011; pp 147–177.

(16) Turan, K.; Örçen, G. Failure Analysis of Adhesive-Patch-Repaired Edge-Notched Composite Plates. *J. Adhes.* **2017**, *93* (4), 328–341. https://doi.org/10.1080/00218464.2015.1116984.

(17) CAMPILHO, R. D. S. G.; DA SILVA, L. F. M. Mode I Fatigue and Fracture Behaviour of Adhesively-Bonded Carbon Fibre-Reinforced Polymer (CFRP) Composite Joints. In *Fatigue and Fracture of Adhesively-Bonded Composite Joints*; 2015; pp 93–120.

(18) Deitzel, J. M.; Kleinmeyer, J.; Harris, D.; Beck Tan, N. C. The Effect of Processing Variables on the Morphology of Electrospun. *Polymer (Guildf).* **2001**, *42*, 261–272.

(19) Fang, X.; Reneker, D. H. DNA Fibers by Electrospinning. *J. Macromol. Sci. - Phys.* **1997**, *36* (2), 169–173. https://doi.org/10.1080/00222349708220422.

(20) Lyons, J.; Li, C.; Ko, F. Melt-Electrospinning Part I: Processing Parameters and Geometric Properties. *Polymer (Guildf).* **2004**, *45* (22), 7597–7603. https://doi.org/10.1016/j.polymer.2004.08.071.

(21) Larrondo, L.; Manley, R. S. J. Electrostatic Fiber Spinning From Polymer Melts - 3. Electrostatic Deformation of a Pendant Drop of Polymer Melt. *J. Polym. Sci. Part A-2, Polym. Phys.* **1981**, *19* (6), 933–940. https://doi.org/10.1002/pol.1981.180190603.

(22) De Freitas, S. T.; Sinke, J. Adhesion Properties of Bonded Composite-to-Aluminium Joints Using Peel Tests. *J. Adhes.* **2014**, *90* (5–6), 511–525. https://doi.org/10.1080/00218464.2013.850424.

(23) Quini, J. G.; Marinucci, G. Polyurethane Structural Adhesives Applied in Automotive Composite Joints. *Mater. Res.* **2012**, *15* (3), 434–439. https://doi.org/10.1590/S1516-14392012005000042.

(24) Reitz, V.; Meinhard, D.; Ruck, S.; Riegel, H.; Knoblauch, V. A Comparison of IR- and UV-Laser Pretreatment to Increase the Bonding Strength of Adhesively Joined Aluminum/CFRP Components. *Compos. Part A Appl. Sci. Manuf.* **2017**, *96*, 18–27. https://doi.org/10.1016/j.compositesa.2017.02.014.

(25) Rauh, B.; Kreling, S.; Kolb, M.; Geistbeck, M.; Boujenfa, S.; Suess, M.; Dilger, K. UV-Laser Cleaning and Surface Characterization of an Aerospace Carbon Fibre Reinforced Polymer. *Int. J. Adhes. Adhes.* **2018**, *82* (December 2017), 50–59. https://doi.org/10.1016/j.ijadhadh.2017.12.016.

(26) Ledesma, R. I.; Palmieri, F. L.; Lin, Y.; Belcher, M. A.; Ferriell, D. R.; Thomas, S. K.; Connell, J. W. Picosecond Laser Surface Treatment and Analysis of Thermoplastic Composites for Structural Adhesive Bonding. *Compos. Part B Eng.* **2020**, *191* (November 2019), 107939. https://doi.org/10.1016/j.compositesb.2020.107939.

(27) Botana-Galvín, M.; Blanco, G.; González-Rovira, L.; Rodríguez, M. A.; Botana, F. J. Adhesive Behaviour of Carbon Fibre Reinforced Plastic Panels Manufactured Using Woven and Unidirectional Tape after Ultraviolet Laser Surface Treatment. *J. Compos. Mater.* **2018**, *52* (7), 853–865. https://doi.org/10.1177/0021998317718614.

(28) Li, Y.; Meng, S.; Gong, Q.; Huang, Y.; Gan, J.; Zhao, M.; Liu, B.; Liu, L.; Zou, G.; Zhuang, D. Experimental and Theoretical Investigation of Laser Pretreatment

on Strengthening the Heterojunction between Carbon Fiber-Reinforced Plastic and Aluminum Alloy. *ACS Applied Materials and Interfaces*. 2019, pp 22005–22014. https://doi.org/10.1021/acsami.9b04080.

(29) Özgür Bora, M.; Çoban, O.; Akman, E.; Oztoprak, B. G.; Kutluk, T. Comparison of Novel Surface Treatments of Al 2024 Alloy for Al/Cfrp Adhesive Bonded Joints. *Int. J. Adhes. Adhes.* **2020**, *103*. https://doi.org/10.1016/j.ijadhadh.2020.102721.

(30) Gao, Q.; Li, Y.; Wang, H. en; Liu, W.; Shen, H.; Zhan, X. Effect of Scanning Speed with UV Laser Cleaning on Adhesive Bonding Tensile Properties of CFRP. *Appl. Compos. Mater.* **2019**, *26* (4), 1087–1099. https://doi.org/10.1007/s10443-019-09768-4.

(31) Li, Y.; Zhan, X.; Gao, C.; Wang, H.; Yang, Y. Comparative Study of Infrared Laser Surface Treatment and Ultraviolet Laser Surface Treatment of CFRP Laminates. *Int. J. Adv. Manuf. Technol.* **2019**, *102* (9–12), 4059–4071. https://doi.org/10.1007/s00170-019-03368-z.

(32) Zhan, X.; Li, Y.; Gao, C.; Wang, H.; Yang, Y. Effect of Infrared Laser Surface Treatment on the Microstructure and Properties of Adhesively CFRP Bonded Joints. *Opt. Laser Technol.* **2018**, *106*, 398–409. https://doi.org/10.1016/j.optlastec.2018.04.023.

(33) Akman, E.; Erdoğan, Y.; Bora, M. Ö.; Çoban, O.; Oztoprak, B. G.; Demir, A. Investigation of the Differences between Photochemical and Photothermal Laser Ablation on the Shear Strength of CFRP/CFRP Adhesive Joints. *Int. J. Adhes. Adhes.* **2020**, *98*. https://doi.org/10.1016/j.ijadhadh.2020.102548.

(34) Loutas, T. H.; Sotiriadis, G.; Tsonos, E.; Psarras, S.; Kostopoulos, V. Investigation of a Pulsed Laser Ablation Process for Bonded Repair Purposes of CFRP Composites via Peel Testing and a Design-of-Experiments Approach. *Int. J. Adhes. Adhes.* **2019**, *95* (July), 102407. https://doi.org/10.1016/j.ijadhadh.2019.102407.

(35) Tao, R.; Alfano, M.; Lubineau, G. Laser-Based Surface Patterning of Composite Plates for Improved Secondary Adhesive Bonding. *Compos. Part A Appl. Sci. Manuf.* **2018**, *109* (February), 84–94. https://doi.org/10.1016/j.compositesa.2018.02.041.

(36) Moreira, R. D. F.; Oliveira, V.; Silva, F. G. A.; Vilar, R.; de Moura, M. F. S. F.

Mode II Fracture Toughness of Carbon–Epoxy Bonded Joints with Femtosecond Laser Treated Surfaces. *Int. J. Mech. Sci.* **2018**, *148* (March), 707–713. https://doi.org/10.1016/j.ijmecsci.2018.09.029.

(37) Banat, D.; Ganguly, S.; Meco, S.; Harrison, P. Application of High Power Pulsed Nanosecond Fibre Lasers in Processing Ultra-Thin Aluminium Foils. *Opt. Lasers Eng.* **2020**, *129* (February). https://doi.org/10.1016/j.optlaseng.2020.106075.

(38) Harder, S.; Schmutzler, H.; Hergoss, P.; Freese, J.; Holtmannspötter, J.; Fiedler, B. Effect of Infrared Laser Surface Treatment on the Morphology and Adhesive Properties of Scarfed CFRP Surfaces. *Compos. Part A Appl. Sci. Manuf.* **2019**, *121* (November 2018), 299–307. https://doi.org/10.1016/j.compositesa.2019.02.025.

(39) ASTM D5528-01. Standard Test Method for Mode I Interlaminar Fracture Toughness of Unidirectional Fiber-Reinforced Polymer Matrix Composites. *Am. Stand. Test. Methods* **2014**, *03* (Reapproved 2007), 1–12. https://doi.org/10.1520/D5528-13.2.